Resonances in low-energy electron elastic cross sections for lanthanide atoms

Z. Felfli,[1] A. Z. Msezane,[1] and D. Sokolovski[2]
[1]*Department of Physics and Centre for Theoretical Studies of Physical Systems, Clark Atlanta University, Atlanta, Georgia 30314, USA*
[2]*School of Mathematics and Physics, Queen's University of Belfast, Belfast, BT7 1NN, United Kingdom*
(Received 6 October 2008; revised manuscript received 4 December 2008; published 27 January 2009)

Total and Mulholland partial cross sections for the elastic scattering of electrons from the lanthanide atoms lanthanum to lutetium are calculated for the electron impact energy range $0 \leqslant E \leqslant 1$ eV. The recently developed Regge-pole methodology, which naturally embodies the crucial electron correlation effects together with a Thomas-Fermi-type potential incorporating the vital core-polarization interaction are used for the calculations. Dramatically sharp resonances are found to characterize the near-threshold electron elastic scattering total and Mulholland partial cross sections, whose energy positions are identified with the electron affinities (EA's) of these atoms through a close scrutiny of the imaginary part of the complex angular momentum. The unambiguous extracted EA values of the lanthanide atoms vary from a low value of 0.016 eV for the Tm atom to a high value of 0.631 eV for the Pr atom; none is predicted to have a lower EA value than the former. All the negative ions of the lanthanide atoms can be classified through their binding energies (BE's) as weakly bound negative ions (BE's <1.0 eV), while only three qualify to be classified as tenuously bound (BE'<0.1 eV). Ramsauer-Townsend minima, shape resonances, and the Wigner threshold behavior for these lanthanides are also determined. Comparisons of the present calculated EA's with those from various experimental measurements and other theoretical calculations are presented and discussed. In particular, our extracted EA value for the complicated open *d*- and *f*-subshell Ce atom agrees excellently with the most recently measured [Walter *et al.*, Phys. Rev. A **76**, 052702 (2007)] and calculated values, while for Nd and Eu the agreement with the latest calculated values of O'Malley and Beck [Phys. Rev. A **77**, 012505 (2008); Phys. Rev. A **78**, 012510 (2008)] is outstanding. These agreements give great credence to the already demonstrated predictive power of the Regge-pole methodology to extract unambiguous and reliable binding energies for tenuously bound and complicated open-shell negative ionic systems, requiring no *a priori* knowledge of the EA values whatsoever. This new perspective to the EA determination of atoms from low-energy electron elastic scattering resonances promises far-reaching implications for future accurate and reliable theoretical EA values, even for small molecules and clusters.

DOI: 10.1103/PhysRevA.79.012714 PACS number(s): 34.80.Bm

I. INTRODUCTION

The main objective of this paper is to investigate the near-threshold resonance structures in the elastic total cross sections (TCS's) and the Mulholland partial cross sections for electron scattering from the lanthanide atoms, La to Lu in the electron impact energy, E range of less than 1 eV and present these cross sections. As a by-product we then extract the electron affinity (EA) values of the lanthanides through the careful scrutiny of the imaginary part of the complex angular momentum L. For the binding energy (BE) of the stable ground state of the negative ion thus formed during the collision as a Regge resonance, also numerically equal to the EA, the imaginary part of L, Im L is several orders of magnitude smaller than the value corresponding to that of the attendant shape resonance.

The motivation of this paper is mainly fourfold: (1) the lack of measured or calculated electron elastic scattering total and/or partial cross sections for the lanthanide atoms near their elastic thresholds, including the identification of the attendant Ramsauer-Townsend (RT) minima, shape resonances, and the Wigner threshold law; (2) the sparse availability of reliable experimental and/or theoretical electron affinity values for the lanthanide atoms; there are even several gaps in the recent tabulation of their EA values; (3) the need for the identification of ground-state atoms with small EA's for application in the quenching of Rydberg states; and (4) the recent successful extraction of binding energies for tenuously bound (BE<0.1 eV), weakly bound (BE<1 eV), and complicated open-shell and strongly bound (BE >1 eV) negative ions from resonances in the near-threshold elastic scattering cross sections obtained using the Regge-pole methodology.

The theoretical prediction [1] and the experimental confirmation [2] of the existence of a stable bound state of the closed-shell Ca^- negative ion, culminating in the current accepted experimental [3,4] value of its electron affinity have inspired considerable investigations involving negative ions for various reasons [5–8]. These measurements are from resonant formation of the Ca^- negative ion in thermal-energy collisions of Rydberg and ground-state Ca atoms [3] and laser photodetachment electron spectroscopy (LPES) [4]. The existence of temporary negative ion states and their properties, represented essentially by shape resonances, are responsible for the mechanism through which low-energy electron scattering deposits energy and induces chemical transitions [9]. Electron-induced chemical processes resulting in nega-

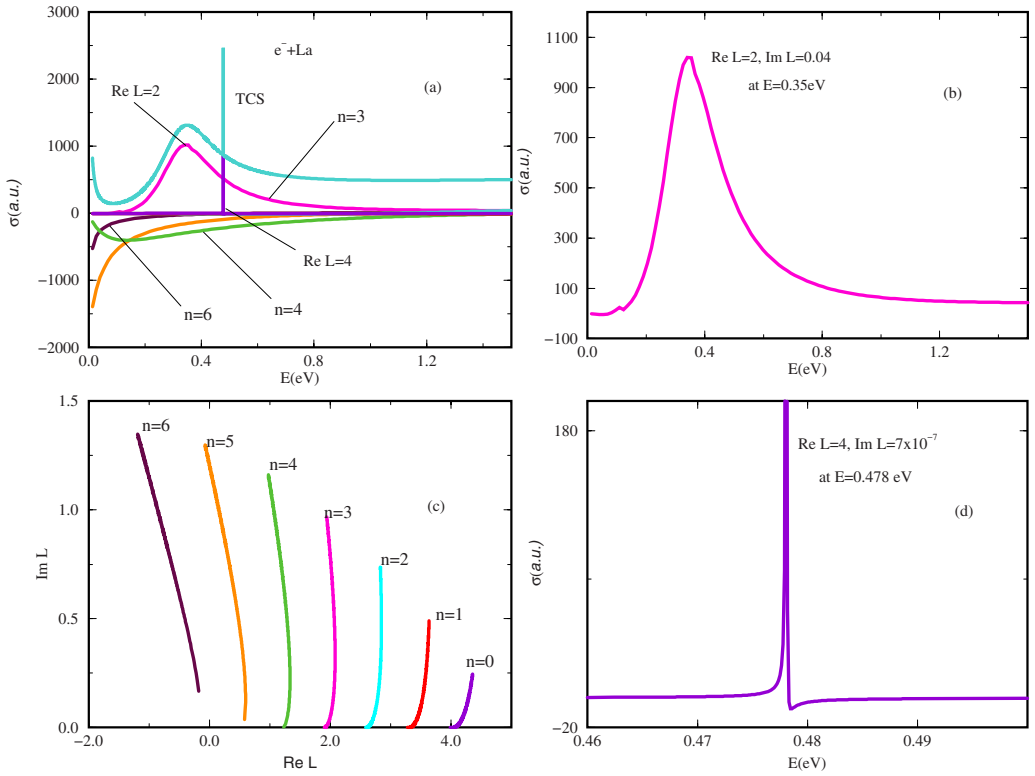

FIG. 1. (Color online) (a) Total and Mulholland partial elastic cross sections, in atomic units, for e^--La scattering versus E (eV), showing the Mulholland contributions. The $n=4$ (green curve) Mulholland partial cross section also determines the Wigner threshold behavior. The RT minimum is clearly visible near threshold. (b) Mulholland contribution to the total cross section, in atomic units, for e^--La scattering versus E (eV), corresponding to the Regge trajectory that passes near $\mathrm{Re}\,L=2$ at $E=0.350$ eV, and hence responsible for the short-lived resonance ($\mathrm{Im}\,L=0.04$) in the TCS at that energy. (c) Regge trajectories, viz., $\mathrm{Im}\,L(E)$ versus $\mathrm{Re}\,L(E)$, for La^-, demonstrating the main $\mathrm{Re}\,L(E)$ contributors to the TCS. (d) Mulholland contribution to the total cross section, in atomic units, for e^--La scattering versus E (eV), corresponding to the Regge trajectory that passes near $\mathrm{Re}\,L=4$ at $E=0.478$ eV, and hence responsible for the resonance ($\mathrm{Im}\,L=7.0\times10^{-7}$) in the TCS at that energy. This is a long-lived resonance as seen from its large angular life $(\mathrm{Im}\,L)^{-1}$ and corresponds to the EA for the La atom.

tive ion production have been interpreted in terms of shape resonances [10]. Resonances in spin-flipping and elastic cross sections are important in selecting molecules for cold and ultracold experiments [11], including their creation [12]. The RT effect plays an essential role in understanding *inter alia* sympathetic cooling and the production of cold molecules from natural fermions [13]. Hence the general need for reliable values for the RT minima and the shape resonances.

The Wigner threshold law [14] is crucial in high-precision measurements of BE's of valence electrons using photodetachment threshold spectroscopy [15]. The quenching of Rydberg atoms through the collisions with ground-state atoms requires that the latter have low EA values as was demonstrated with the Ca^- negative ion [3,16,17]. The search for atoms with low EA's is also a reason for the present investigation of the low-energy electron scattering from the lanthanide atoms. A thorough investigation and understanding of the structure and dynamics of very low-energy electron elastic scattering from the lanthanide atoms are also needed because of their important role in heavy-fermion metals and heavy-fermion compounds. These are many Ce, Yb, U, etc. compounds with localized f electrons. Their existence is attributed to the presence of the partly filled f orbital of the rare-earth-metal or actinide ions, causing them to behave like localized magnetic moments [18]. Examples are $CeCu_6$, $CeAl_3$, $YbIr_2Si_2$, and UPd_2Al_3. The most attractive and elusive phenomenon of the heavy-fermion systems is the appearance of superconductivity in a few compounds such as $CeCu_2Si_2$. Additionally, the rare-earth-metal monosulfides such as LaS, ErS, EuS, GdS, etc. at various III-V semiconductor surfaces offer attractive possibilities of reaching negative electron affinities [19]. A recent density functional theory (DFT) study of the evolution of Pt^- negative ion clusters concluded that when the cluster size was less than about 5, corresponding to atomic behavior, agreement between theory and measurement on the EA was out by a factor of 2. However, as the cluster size increased beyond 5, the agreement became excellent [20]. This is a clear manifestation of the different fundamental physics operating at the different length scales.

Davis *et al.* [21] have determined the EA's of several of the lanthanide atoms using laser photodetachment electron spectroscopy (LPES) experiments and inferred the limits on the EA's of the remaining lanthanides. They also compared their determined EA's with values measured or estimated by accelerator mass spectroscopy (AMS), electric field disassociation (EFD), and laser photodetachment resonant ioniza-

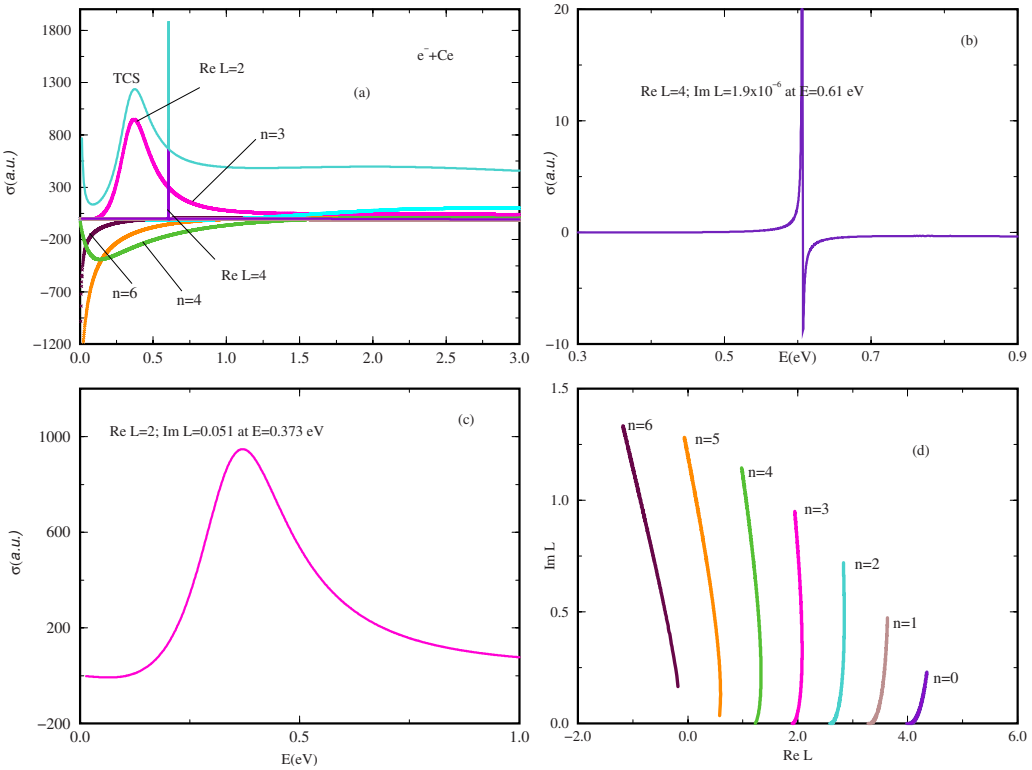

FIG. 2. (Color online) (a) The same as in Fig. 1(a) except that the results are for e^--Ce scattering versus E (eV). Note the Wigner threshold behavior of the TCS, which clearly is determined by the $n=6$ Mulholland partial cross section and the RT minimum near threshold as well. (b) The same as in Fig. 1(d) except that the results are for e^--Ce scattering versus E (eV), corresponding to the Regge trajectory that passes near Re $L=4$ at $E=0.61$ eV, and hence responsible for the resonance (Im $L=1.9\times10^{-6}$) in the TCS at that energy. This is a long-lived resonance as seen by its large angular life $(\text{Im}\,L)^{-1}$. (c) The same as in Fig. 1(b) except that the results are for e^--Ce scattering versus E (eV), corresponding to the Regge trajectory that passes near Re $L=2$ at $E=0.37$ eV, and hence responsible for the resonance (Im $L=0.05$) in the TCS at that energy. This is a short-lived resonance as seen from its large angular life $(\text{Im}\,L)^{-1}$. (d) Regge trajectories, viz., Im $L(E)$ versus Re $L(E)$, for Ce^-, demonstrating the main Re $L(E)$ contributors to the TCS.

tion (LPRI) experimental methods [21–32] and calculated using various sophisticated theoretical methods [33–51]. Hitherto, because of its highly radioactive nature, the negative ion Pm^- had never been studied either experimentally or theoretically; its present calculated cross sections and EA value are thus the first ever. There is a significant number (more than half) of the lanthanide atoms whose EA values have not been investigated theoretically. They are Pm, Sm, Eu, Gd, Tb, Dy, Ho, and Er. The reason is that complex and subtle interactions among the many diverse electron configurations in the lanthanide atoms render accurate and reliable structure-based-type calculations very difficult, if not impossible.

The most interesting and intriguing negative ion among the lanthanides in the context of its EA determination is Yb^-. Andersen *et al.* [52] concluded from their LPRI experimental investigation that a stable bound state Yb^-, if it exists, must have a BE of less than 3 meV. However, the experiment of Nadeau *et al.* [24] obtained the approximate value of 0.010 eV for its EA and previous theoretical calculations determined that a stable negative ion of Yb^- existed [41,42,50]. But Dzuba and Gribakin [49] subsequently contradicted their previous prediction [47] and concluded that the lowest negative ion state Yb^- $4f^{14}6s6p\ ^2P_{1/2}$ is a low-lying shape resonance rather than a bound state. These authors make a very important fundamental point, viz., "none of the theoretical approaches could produce true *ab initio* BE's with meV accuracy." Interestingly, the measurement of Davis *et al.* [21] focused on a possible bound S state of Yb^-, while Andersen *et al.* [52] and Dzuba and Gribakin [49] concentrated on the possible existence of a bound P state of the negative Yb^- ion. Consequently, the conclusions by these investigators [21,49,52] may be valid only under the assumed electron attachment conditions.

On the contrary our study predicts from electron-Yb scattering resonances a stable bound state of the Yb^- ion. Consequently, as far as we are concerned the case of the existence of a stable Yb^- negative ion bound state is still an open question. The Ce^- and Gd^- negative ions are the most complicated of the lanthanides in the context of both having open f and d subshells. Very recently, the EA of Ce has been measured [53] and calculated [36,54], with the calculations obtaining very good agreement with the measurement. Additionally, excellent agreement has been realized between the O'Malley and Beck [55] EA for Nd and our present Regge-pole value.

In this paper we explore electron-lanthanide atom scattering in the near-threshold energy region using the recently developed nonrelativistic Regge-pole methodology [56] wherein is inherent the crucial electron-electron correlations,

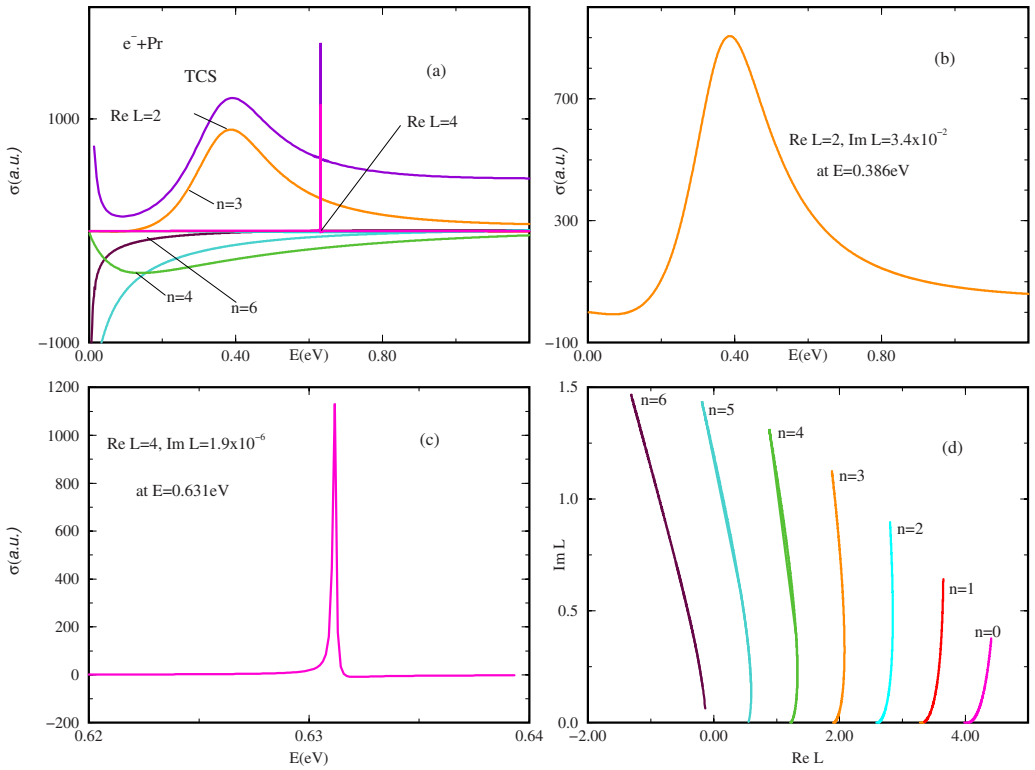

FIG. 3. (Color online) (a) The same as in Fig. 1(a) except that the results are for e^--Pr scattering versus E (eV). Note the Wigner threshold behavior of the TCS, which clearly is determined by the $n=4$ Mulholland partial cross section as well as the RT minimum near threshold. (b) The same as in Fig. 1(b) except that the results are for e^--Pr scattering versus E (eV), corresponding to the Regge trajectory that passes near Re $L=2$ at $E=0.386$ eV, and hence responsible for the short-lived resonance (Im $L=3.4\times10^{-2}$) in the TCS at that energy. (c) The same as in Fig. 1(d) except that the results are for e^--Pr scattering versus E (eV), corresponding to the Regge trajectory that passes near Re $L=4$ at $E=0.631$ eV, and hence responsible for the resonance (Im $L=1.9\times10^{-6}$) in the TCS at that energy. This is a long-lived resonance as seen by its large angular life $(\mathrm{Im}\,L)^{-1}$. (d) Regge trajectories, viz., Im $L(E)$ versus Re $L(E)$, for Pr^-, demonstrating the main Re $L(E)$ contributors to the TCS.

which together with the vital core-polarization interaction, incorporated within the Thomas-Fermi (TF) type potential used here, are responsible for the stability of the bound states of the negative ions. We search for subtle behaviors exhibited through dramatically sharp long-lived resonances in the elastic total cross sections, identifiable mainly through the careful scrutiny of the imaginary part of the complex angular momentum (CAM), L. These resonances have been identified as the signatures of the stable bound states of the negative ions formed during the collisions. RT minima, shape resonances, and the Wigner threshold law are also determined. The Regge-pole methodology is appropriate for the investigation since Regge poles, singularities of the S matrix, rigorously define resonances [57,58].

The structure of the paper is as follows. Sections II and III present the Calculational Procedure and the Results, respectively. The Summary and Conclusions are presented in Sec. IV.

II. CALCULATIONAL PROCEDURE

The Regge analysis has been employed successfully in heavy particle collisions [59], electron-atom scattering [54,56,60–63], and resonance reactive scattering [64,65] to understand the oscillations in the elastic total scattering cross sections in the near-threshold energy region, including the dramatically sharp resonances in both the TCS's and DCS's for low-energy electron elastic scattering by Hf and Lu atoms [66], whose energy positions have been identified with their EA's. Various theoretical investigations have demonstrated through comparisons with measurements the crucial importance of the polarization interaction in low-energy electron scattering from atoms and molecules [67–72]. Because of neglect of the vital polarization interaction a recent 23-state fully relativistic R-matrix calculation failed to reduce the factor of about 2 discrepancy between the measured [69] and the calculated [70] EA value for the Ba atom.

For the investigation of the near-threshold scattering cross sections the Mulholland formula [73], implemented within the CAM representation of scattering, is employed in the form [56,59] (atomic units are used throughout)

$$\sigma_{tot}(E) = 4\pi k^{-2}\int_0^\infty \mathrm{Re}[1-S(\lambda)]\lambda d\lambda - 8\pi^2 k^{-2}\sum_n \mathrm{Im}\frac{\lambda_n\rho_n}{1+\exp(-2\pi i\lambda_n)} + I(E), \quad (1)$$

where S is the S matrix, $k=\sqrt{(2mE)}$, with m being the mass, ρ_n the residue of the S matrix at the nth pole λ_n, and $I(E)$

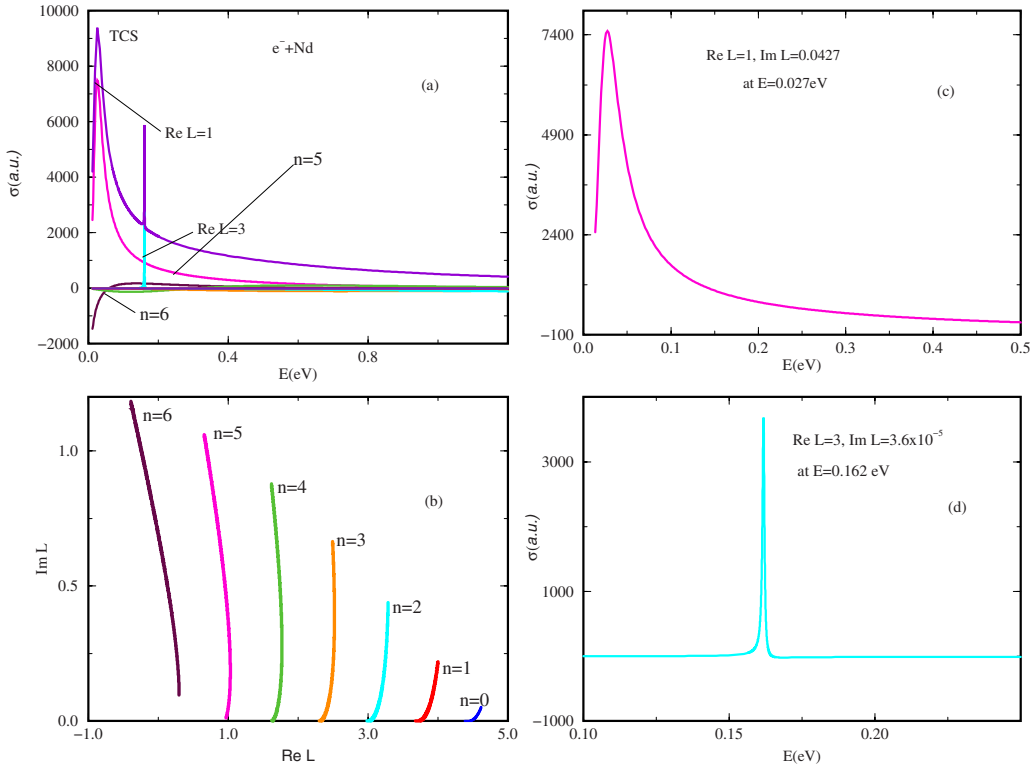

FIG. 4. (Color online) (a) The same as in Fig. 1(a) except that the results are for e^--Nd scattering versus E (eV); note the pronounced maximum near threshold in the TCS, which is dominated by a Mulholland partial cross section corresponding to Re $L=1$. (b) Regge trajectories, viz., Im $L(E)$ versus Re $L(E)$, for Nd^-, demonstrating the main Re $L(E)$ contributors to the TCS. (c) The same as in Fig. 1(b) except that the results are for e^--Nd scattering versus E (eV), corresponding to the Regge trajectory that passes near Re $L=1$ at $E=0.027$ eV, and hence responsible for the short-lived resonance (Im $L=0.0427$) in the TCS at that energy. (d) The same as in Fig. 1(d) except that the results are for e^--Nd scattering versus E (eV), corresponding to the Regge trajectory that passes near Re $L=3$ at $E=0.162$ eV, and hence responsible for the resonance (Im $L=3.6\times10^{-5}$) in the TCS at that energy. This is a long-lived resonance as seen by its large angular life $(\text{Im}\, L)^{-1}$.

contains the contributions from the integrals along the imaginary λ axis. If the lifetime of the complex is sufficiently long for the complex to return to the forward direction many times, then Im $\lambda_n \ll 1$ must be satisfied, and for constructive addition, Re $\lambda_n \approx 1/2, 3/2, 5/2 \ldots$ or Re $L \cong 0, 1, 2 \ldots$. Thus the importance of Eq. (1) is that a resonance is likely to affect the elastic TCS when its Regge pole position is close to a real integer; see further details in [56], and references therein.

In the present work we employ the well investigated form of the TF [74] potential [75]

$$U(r) = \frac{-Z}{r(1+aZ^{1/3}r)(1+bZ^{2/3}r^2)}, \tag{2}$$

where Z is the nuclear charge and a and b are adjustable parameters. For small r, the potential describes the Coulomb attraction between an electron and a nucleus, $U(r) \sim -Z/r$, while at large distances it mimics the polarization potential, $U(r) \sim -1/(abr^4)$ and accounts properly for the vital polarization interaction at very low energies, the energy region of our interest. The effective potential

$$V(r) = U(r) + L(L+1)/(2r^2) \tag{3}$$

is considered here as a continuous function of the variables r and L. For $L=0$, $V(r)$ is a potential well which, due to its short-ranged, $\sim 1/r^4$, asymptotic behavior supports a finite number of bound states [56]. As the centrifugal barrier is added to $U(r)$ the well becomes shallower, and the bound states move upwards and are eventually squeezed into the continuum. For larger L's the effective potential develops a barrier. Consequently, a bound state crossing the threshold energy $E=0$ in this region may continue to be separated by a barrier, i.e., becomes a long-lived metastable state. It would continue that way until it passes the barrier top. For larger L values, $V(r)$ becomes purely repulsive so that it no longer can support narrow resonances. Plotting Im $L_n(E)$ versus Re $L_n(E)$ the well known Regge trajectories can be investigated [76]. The S matrix, poles positions, and residues in Eq. (1) were evaluated following a method similar to that of Burke and Tate [77].

The importance of Im L in distinguishing between the shape resonances (short-lived resonances) and the stable bound states of the negative ions (long-lived resonances) formed as Regge resonances in the electron-atom scattering, follows from the definitions of Connor [76] and the description in [66]. In these references the physical interpretation of $L_n^{(i)} \equiv \text{Im}\, L_n(E)$ is given, namely, a small $L_n^{(i)}$ implies that the system orbits many times before decaying, while a large $L_n^{(i)}$ value denotes a short-lived state. For a true bound state $L_n^{(i)} \equiv 0$ and therefore the angular life, $1/L_n^{(i)} \to \infty$, implying that the system can never decay. We limit our calculation of the

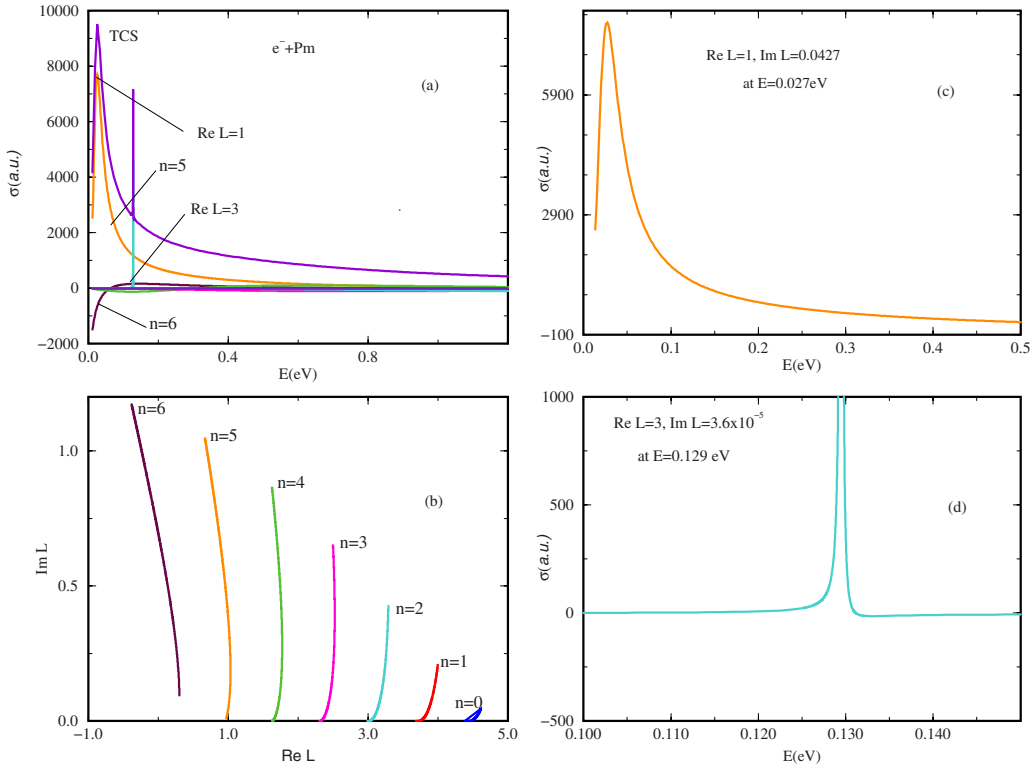

FIG. 5. (Color online) (a) The same as in Fig. 1(a) except that the results are for e^--Pm scattering versus E (eV); note the pronounced maximum near threshold in the TCS, which is dominated by a Mulholland partial cross section corresponding to Re $L=1$. (b) Regge trajectories, viz., Im $L(E)$ versus Re $L(E)$, for Pm^-, demonstrating the main Re $L(E)$ contributors to the TCS. (c) The same as in Fig. 1(b) except that the results are for e^--Pm scattering versus E (eV), corresponding to the Regge trajectory that passes near Re $L=1$ at $E=0.027$ eV, and hence responsible for the short-lived resonance (Im $L=0.0427$) in the TCS at that energy. (d) The same as in Fig. 1(d) except that the results are for e^--Pm scattering versus E (eV), corresponding to the Regge trajectory that passes near Re $L=3$ at $E=0.129$ eV, and hence responsible for the resonance (Im $L=3.6\times10^{-5}$) in the TCS at that energy. This is a long-lived resonance as seen by its large angular life $(\text{Im}\, L)^{-1}$.

cross sections to the near-threshold energy region, namely, below any excitation thresholds to avoid their effects.

When the TCS as a function of "b" has a resonance corresponding to the formation of a negative ion, this resonance is longest lived for a given value of the energy, which corresponds to the electron affinity of the system; this was found to be the case for all of the systems we have investigated so far. Reliable BE's for tenuously bound and complicated open-shell negative ionic systems have been obtained, requiring no *a priori* knowledge of the EA values whatsoever. This fixes the optimal value of "b" for the TF potential used in the calculations of Regge trajectories and the Mulholland partial contributions to the total cross sections.

III. RESULTS

The cross sections are presented in order of ascending atomic number Z of the lanthanides, for convenience. Table I gives the calculated electron affinities, the shape resonances, and the Ramsauer-Towsend minima of the 15 lanthanide atoms. Also included are the values of the b parameter of Eq. (2) for each atom; the value of a is fixed at 0.2 for all of them.

A. Electron scattering from the La atom

Figure 1(a) presents the elastic TCS and the Mulholland partial cross sections versus E (eV) for e^--La scattering. Apart from the maximum at threshold followed by a RT minimum at about 0.087 eV, there are two additional resonances at 0.350 and 0.478 eV, with Re $L=2$ and Re $L=4$, respectively. The corresponding Im L values are, respectively, 4.0×10^{-2} and 7.0×10^{-7}. Clearly, the latter corresponds to a long-lived state, a bound state of the La^- negative ion since the angular life is proportional to $1/(\text{Im}\, L)$, while the former represents a short-lived resonance; in this case it is a shape resonance. The RT minimum at 0.087 eV is generated through the interference between the $n=3$ and $n=4$ Mulholland partial cross sections; the latter also determines the Wigner threshold behavior. We note that this value differs from the true RT minimum, defined by where the $n=6$ Mulholland partial cross section crosses the real axis. Figure 1(b) displays the magnified shape resonance at 0.350 eV, corresponding to Re $L=2$ and Im $L=0.04$. Note the significant difference between the angular lives of the shape resonance and the stable bound state of the La^- negative ion [see also Fig. 1(d)].

Figure 1(c) displays the Regge trajectories, demonstrating that indeed the $n=3$ trajectory at Re $L=2$ is responsible for the resonance at 0.350 eV, while the $n=0$ trajectory with Re $L=4$ accounts for the very sharp resonance at 0.478 eV; these trajectories are close to integer values of Re L. We note that this resonance can easily be missed in both calculations and measurements because it is so narrow. A closer look at

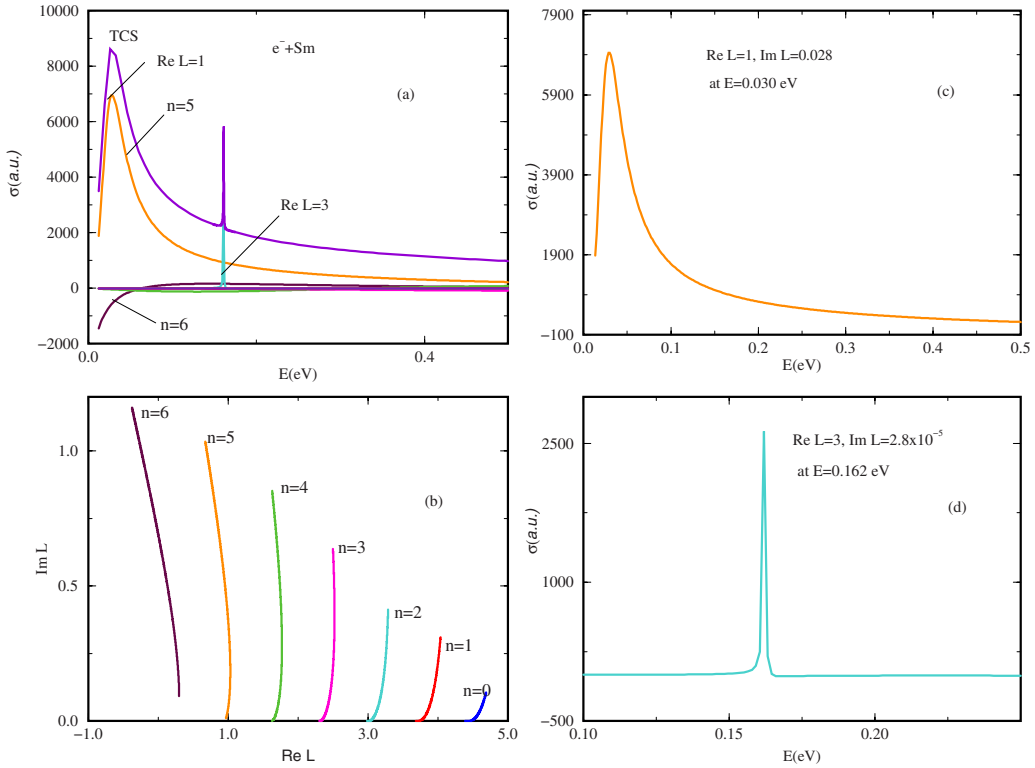

FIG. 6. (Color online) (a) The same as in Fig. 1(a) except that the results are for e^--Sm scattering versus E (eV); note the pronounced maximum near threshold in the TCS, which is dominated by a Mulholland partial cross section corresponding to Re $L=1$. (b) Regge trajectories, viz., Im $L(E)$ versus Re $L(E)$, for Sm^-, demonstrating the main Re $L(E)$ contributors to the TCS. (c) The same as in Fig. 1(b) except that the results are for e^--Sm scattering versus E (eV), corresponding to the Regge trajectory that passes near Re $L=1$ at $E=0.030$ eV, and hence responsible for the short-lived resonance (Im $L=0.028$) in the TCS at that energy. (d) The same as in Fig. 1(d) except that the results are for e^--Sm scattering versus E (eV), corresponding to the Regge trajectory that passes near Re $L=3$ at $E=0.162$ eV, and hence responsible for the resonance (Im $L=2.8\times10^{-5}$) in the TCS at that energy. This is a long-lived resonance as seen by its large angular life $(\text{Im}\, L)^{-1}$.

the bound state of the La^- ion is given in the expanded Fig. 1(d). The values for this resonance at 0.478 eV and Re $L=4$ should be compared with the measured [26,27] and the calculated [43,46] ones. Our EA value agrees excellently with the measured value $(0.47\pm0.02$ eV) [27] and well with the lower limit estimate [26]. The theoretical values [43,46] underestimate the present and the measured EA values.

B. Electron scattering from the Ce atom

The analysis of the near-threshold resonance structures in the cross sections for the e^--Ce scattering, displayed in Fig. 2(a), is essentially the same as for the e^--La scattering and some of the results have already been published elsewhere [54]. The positions of the first and second maxima in the e^--Ce scattering are at the E values of 0.373 and 0.610 eV, respectively. For the former shape resonance Re $L=2$ and Im $L=0.051$, while the values Re $L=4$ and Im $L=1.9\times10^{-6}$ are for the latter. As in Fig. 1 the second resonance corresponds to the binding energy of the Ce^- negative ion formed during the collision since its angular life is significantly larger than that of the first resonance. These resonances are appropriately displayed in Figs. 2(c) and 2(b). Several measurements and theoretical calculations of the EA of Ce are available for comparisons as exhibited in Table II. Essentially, the present calculated EA for the Ce atom agrees very well with the most recently measured value [53], but disagrees significantly with that of Davis and Thompson [30]. Also, agreement is very good with the calculated value of O'Malley and Beck [36] and moderate with the earlier calculation of Cao and Dolg [35]; see also comparisons in Table II.

We note that the general interest in these previous measurements and calculations has been on the EA value of the Ce atom, hence the absence of other data near threshold. The Wigner threshold behavior is determined by the $n=4$ Mulholland partial cross section while the RT minimum is at about 0.088 eV, also formed through the interference between the $n=3$ and the $n=4$ Mulholland partial cross sections. Figure 2(d) gives the Regge trajectories, demonstrating that indeed the $n=3$ trajectory with Re $L=2$ is responsible for the resonance at 0.373 eV, while the $n=0$ trajectory with Re $L=4$ accounts for the very sharp resonance at 0.610 eV, corresponding to the stable bound state of the Ce^- ion.

C. Electron scattering from the Pr atom

The behavior, also quite similar to that of Fig. 1, of the near-threshold electron elastic scattering TCS and the Mulholland partial cross sections for the e^--Pr scattering as func-

TABLE I. Calculated electron affinities [EA's (eV)], shape resonances [SR's (eV)], Ramsauer-Townsend (RT), minima (eV), and b parameter for the lanthanide atoms.

Z	Symbol	b parameter	EA	Re L	Im L	SR	Re L	Im L	RT minimum
57	La	0.0452	0.478	4	7.8×10^{-7}	0.350	2	0.040	0.087
58	Ce	0.0470	0.610	4	1.9×10^{-6}	0.373	2	0.051	0.088
59	Pr	0.0487	0.631	4	1.9×10^{-6}	0.386	2	0.034	0.088
60	Nd	0.0340	0.162	3	3.6×10^{-5}	0.027	1	0.043	
61	Pm	0.0351	0.129	3	1.4×10^{-5}	0.027	1	0.042	
62	Sm	0.0364	0.162	3	2.8×10^{-5}	0.030	1	0.028	
63	Eu	0.0375	0.116	3	7.6×10^{-6}	0.029	1	0.025	
64	Gd	0.0388	0.137	3	1.2×10^{-5}	0.034	1	0.030	
65	Tb	0.0303	0.436	4	5.0×10^{-6}	0.231	2	0.032	0.068
66	Dy	0.0312	0.352	4	1.6×10^{-6}	0.194	2	0.027	0.068
67	Ho	0.0322	0.338	4	1.1×10^{-6}	0.231	2	0.028	0.070
68	Er	0.0332	0.312	4	6.7×10^{-7}	0.204	2	0.028	0.075
69	Tm	0.0320	0.016	2	3.4×10^{-5}				0.014
70	Yb	0.0331	0.028	2	1.3×10^{-4}				0.024
71	Lu	0.0341	0.029	2	1.4×10^{-4}				0.025

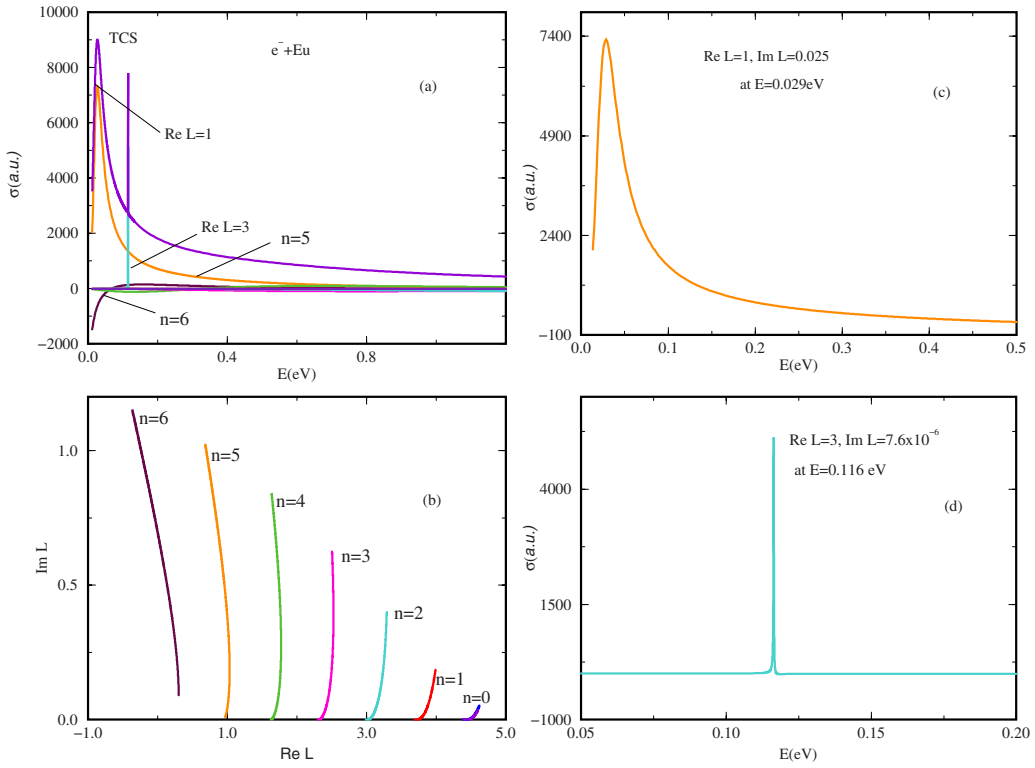

FIG. 7. (Color online) (a) The same as in Fig. 1(a) except that the results are for e^--Eu scattering versus E (eV); note the pronounced maximum near threshold in the TCS which is dominated by a Mulholland partial cross section corresponding to Re $L=1$. (b) Regge trajectories, viz., Im $L(E)$ versus Re $L(E)$, for Eu^-, demonstrating the main Re $L(E)$ contributors to the TCS. (c) The same as in Fig. 1(b) except that the results are for e^--Eu scattering versus E (eV), corresponding to the Regge trajectory that passes near Re $L=1$ at $E=0.029$ eV, and hence responsible for the short-lived resonance (Im $L=0.025$) in the TCS at that energy. (d) The same as in Fig. 1(d) except that the results are for e^--Eu scattering versus E (eV), corresponding to the Regge trajectory that passes near Re $L=3$ at $E=0.116$ eV, and hence responsible for the resonance (Im $L=7.6\times10^{-6}$) in the TCS at that energy. This is a long-lived resonance as seen by its large angular life $(\text{Im } L)^{-1}$.

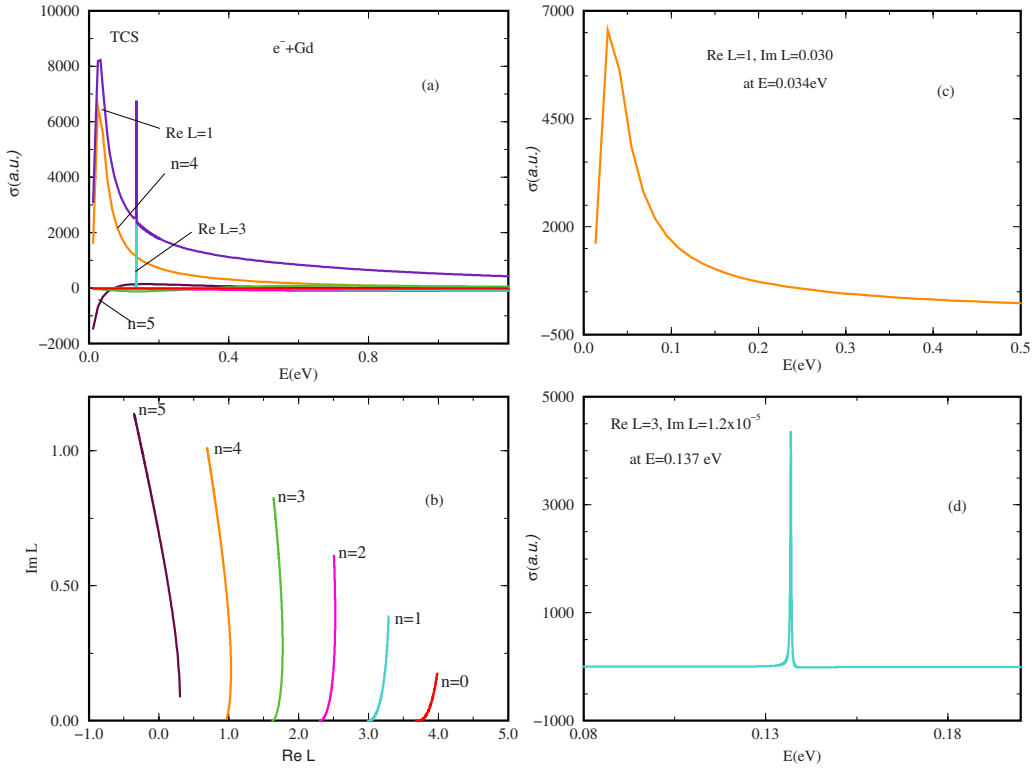

FIG. 8. (Color online) (a) The same as in Fig. 1(a) except that the results are for e^--Gd scattering versus E (eV); note the pronounced maximum near threshold in the TCS, which is dominated by a Mulholland partial cross section corresponding to Re $L=1$. (b) Regge trajectories, viz., Im $L(E)$ versus Re $L(E)$, for Gd^-, demonstrating the main Re $L(E)$ contributors to the TCS. (c) The same as in Fig. 1(b) except that the results are for e^--Gd scattering versus E (eV), corresponding to the Regge trajectory that passes near Re $L=1$ at $E=0.034$ eV, and hence responsible for the short-lived resonance (Im $L=0.030$) in the TCS at that energy. (d) The same as in Fig. 1(d) except that the results are for e^--Gd scattering versus E (eV), corresponding to the Regge trajectory that passes near Re $L=3$ at $E=0.137$ eV, and hence responsible for the resonance (Im $L=1.2\times10^{-5}$) in the TCS at that energy. This is a long-lived resonance as seen by its large angular life $(\text{Im}\, L)^{-1}$.

tions of E (eV) is presented in Fig. 3. Here the RT minimum is also found to be at 0.088 eV, formed through the interference between the $n=3$ and $n=4$ Mulholland partial cross sections, while the Wigner threshold behavior corresponds to the $n=4$ Mulholland partial cross section. For the same reasons given for the e^--La scattering in Fig. 1 the resonance corresponding to the Re $L=2$ and the Im $L=3.4\times10^{-2}$ at 0.386 eV [see Fig. 3(b)], corresponds to a shape resonance. The resonance in Fig. 3(c) with Re $L=4$, Im $L=1.9\times10^{-6}$ at $E=0.631$ eV is identified with the stable ground state of the Pr^- negative ion. This EA value of 0.631 eV should be compared with those in Table II, particularly the measured value of 0.962(24) eV by Davis and Thompson [31], which like in the case of Ce is significantly higher than the rest of the EA values, including the calculated value of 0.128 eV [38]. The Regge trajectories, viz., Im L versus Re L are displayed in Fig. 3(d), demonstrating that indeed the $n=3$ trajectory at Re $L=2$ and the $n=0$ trajectory at Re $L=4$ are responsible for the resonances in Figs. 3(b) and 3(c), respectively.

D. Electron scattering from the Nd atom

The characteristic two pronounced resonances near threshold with energies of 0.027 and 0.162 eV, respectively, are clearly visible in the near-threshold e^--Nd scattering. Note, however, the significantly low value of the shape resonance energy in the e^--Nd scattering as well as its low EA value [see the expanded Figs. 4(c) and 4(d), respectively] in comparison with those of the e^--La, e^--Ce, and e^--Pr scattering. Also, here the RT minimum is much deeper into the near-threshold energy region in comparison with that of the e^--La scattering case, for example. We did not pursue its location since it is not the focus of this paper. In Fig. 4 we also see the introduction of a different Re L attachment value in comparison with the previous cases in which the attachment was to the Re $L=3$. It is difficult to determine the reason for the change by merely examining the structure of the lanthanides, since the d orbitals are mixed intricately with the f orbitals. Nonetheless, we need to remember the importance of the core-polarization interaction, determined mainly by the b parameter (see Table I).

For the Nd atom our calculated value is in excellent agreement with the EA value of O'Malley and Beck [55], but disagrees very strongly with the lower limit of the EA >1.916 eV obtained by the measurement of Davis and Thompson [21] (see Table II for the comparisons). The Regge trajectories for the e^--Nd scattering are plotted in Fig. 4(b), showing that the trajectories ($n=5$ and $n=2$) passing near Re $L=1$ and Re $L=3$ are, respectively, responsible for the shape resonance and the bound state of the negative Nd^- ion.

TABLE II. Comparison of electron affinities (eV) for the lanthanide atoms. LPES denotes laser photoelectron spectroscopy. All EA's are given in eV.

Element	Present	LPES	Other studies
La	0.48	0.470(20) [27]	>0.5 (AMS)[a] [26] 0.27–0.41 (DFT)[b] [46] 0.33 (RCCSD)[c] [43]
Ce	0.61	0.955(26) [30]	0.428 (MCDF-RCI)[d] [37] 0.265 (MCDF-RCI) [51] >0.5 (AMS) [26] 0.7 (AMS) [25] 0.528 (MRCI)[e] [35] 0.660 (MCDF-RCI) [36] 0.65 (3) [53] 0.61 (RP)[f] [54]
Pr	0.631	0.962(24) [31]	0.128 (MCDF-RCI) [38] >0.1 (AMS) [26] 0.177 [78]
Nd	0.162	>1.916	>0.05 (AMS) [26] 0.169 (MCDF-RCI) [55] 0.167 [78]
Pm	0.129	Not studied	0.154 [78]
Sm	0.162		>0.05 (AMS) [26] 0.130 [78]
Eu	0.116	1.053(25) [32]	>0.05 (AMS) [26] 0.117 [78]
Gd	0.137		>0.1 (AMS) [26]
Tb	0.436	>1.165	>0.1 (AMS) [26] 0.085 [78]
Dy	0.352	>0	0.015(3) (EFD)[g] [24] 0.063 [78]
Ho	0.338		>0.005 (EFD) (24) 0.050 [78]
Er	0.312		>0.005 (EFD) (24) 0.038 [78]
Tm	0.016	1.029(22) [28]	0.027–0.136 (DHF-DFT)[h] [39] 0.032(7) (EFD) [24] 0.022 [78]
Yb	0.028	Not bound	Detected (EFD) [24] 0.054(27) (DFT) [41] 0.0985 (CI)[i] [42] 0.001 (DHF)[j] [50] <0.0 (MBT)[k] [49] 0.036 (RCCSD) [47] <0.003 (LPRI)[l] [52]
Lu	0.029	0.346(14) [29]	0.190(100) (DHF-DFT) [45] 0.257 (RCCSD) [43] >0.1 (AMS) [26]

[a]AMS denotes accelerator mass spectroscopy.
[b]DFT denotes density functional theory.
[c]RCCSD=denotes relativistic coupled cluster theory with single and double excitations.
[d]MCDF-RCI denotes multi configurational Dirac-Fock-relativistic configuration interaction.
[e]MRCI denotes multireference configuration-interaction.
[f]RP denotes Regge-Pole analysis.
[g]EFD denotes electric field disassociation.
[h]DHF-DFT denotes Dirac-Hartree-Fock-density functional theory.
[i]CI denotes configuration interaction.
[j]DHF denotes Dirac-Hartree-Fock theory.
[k]MBT denotes many-body theory.
[l]LPRI denotes laser photodetachment resonant ionization.

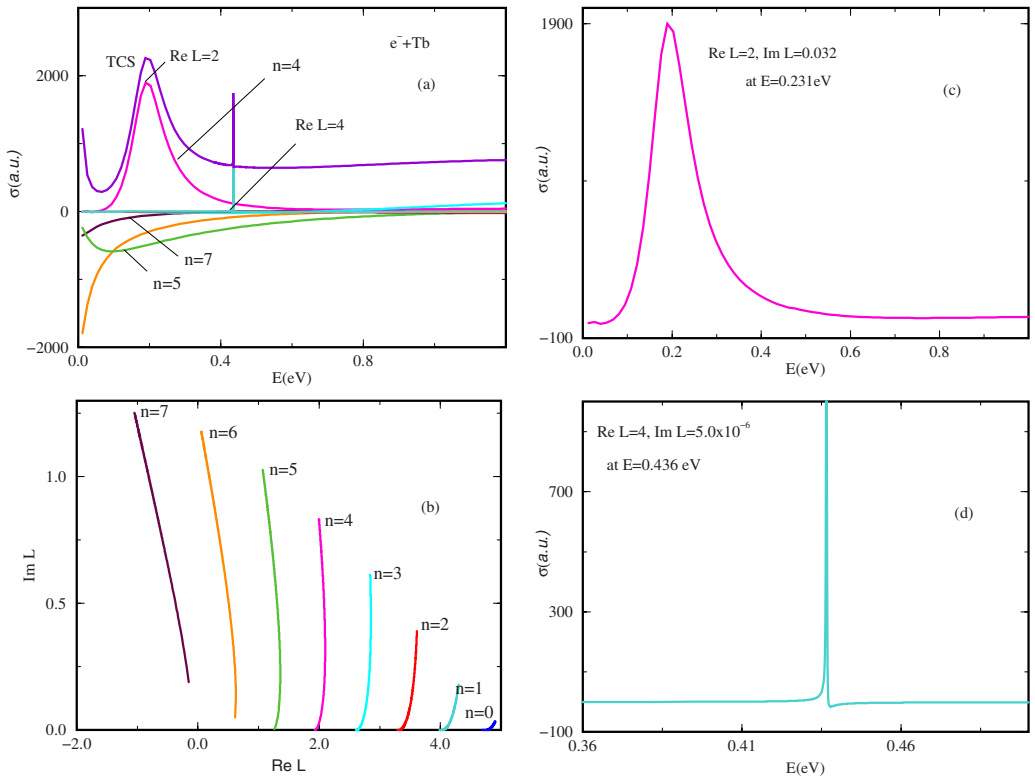

FIG. 9. (Color online) (a) The same as in Fig. 1(a) except that the results are for e^--Tb scattering versus E (eV). Note the Wigner threshold behavior of the TCS, which clearly is determined by the $n=5$ Mulholland partial cross section and the RT minimum near threshold. Figure (b) Regge trajectories, viz., Im $L(E)$ versus Re $L(E)$, for Tb^-, demonstrating the main Re $L(E)$ contributors to the TCS. (c) The same as in Fig. 1(b) except that the results are for e^--Tb scattering versus E (eV), corresponding to the Regge trajectory that passes near Re $L=2$ at $E=0.231$ eV, and hence responsible for the short-lived resonance (Im $L=0.032$) in the TCS at that energy. (d) The same as in Fig. 1(d) except that the results are for e^--Tb scattering versus E (eV), corresponding to the Regge trajectory that passes near Re $L=4$ at $E=0.436$ eV, and hence responsible for the resonance (Im $L=5.0\times10^{-6}$) in the TCS at that energy. This is a long-lived resonance as seen by its large angular life $(\text{Im } L)^{-1}$.

E. Electron scattering from the Pm atom

The near-threshold electron elastic scattering TCS and the Mulholland partial cross sections for the e^--Pm scattering as functions of E (eV) are shown in Fig. 5. They closely resemble those of the e^--Nd scattering, shown in Fig. 4. Furthermore, the e^--Pm scattering resonances appear at lower values of the energy in comparison with those of Figs. 1–3. Figure 5(c) shows the expanded shape resonance whose Re L and Im L values are, respectively, 1 and 0.0427 and the energy is 0.027 eV. Figure 5(d) displays the Mulholland contribution to the total cross section, in a.u., for the e^--Pm scattering versus E (eV), corresponding to the Regge trajectory that passes near Re $L=3$ [see Fig. 5(b)] at $E=0.129$ eV. Thus it is responsible for the resonance in the TCS at that energy. This long-lived resonance, determined from its large angular life, corresponds to the EA for the Pm atom. Its values are Re $L=3$, Im $L=3.6\times10^{-5}$, and EA $=0.129$ eV. We note that there are neither experimental values nor other theoretical values available to compare with. So, this is one of the atoms with not too low an EA value to create serious problems for experiments. Figure 5(b) displays the Regge trajectories, showing the relevant ones to the shape resonance and the bound state of the negative Pm^- ion.

F. Electron scattering from the Sm atom

As seen from Fig. 6(a) the TCS and the Mulholland partial cross sections for the e^--Sm scattering as functions of E (eV) closely resemble those of the e^--Pm scattering. The shape resonance, shown in the expanded view of Fig. 6(c) has Re $L=1$, Im $L=0.028$, and the E value of 0.030 eV. The Mulholland contribution to the total cross section, in a.u., for the e^--Sm scattering versus E (eV), corresponding to the Regge trajectory that passes near Re $L=3$ [see Fig. 6(b)] at $E=0.162$ eV is shown in the expanded Fig. 6(d). This Mulholland contribution is responsible for the resonance in the TCS at that energy. As in the previous cases, this long-lived resonance, determined from its large angular life, namely, $[\text{Im } L=2.8\times10^{-5}]^{-1}$ when compared with that of Fig. 6(c), is identified with the EA of the Sm atom. The only published EA value for the Sm atom to compare with is the lower limit estimate value of 0.05 eV [26] (see Table II). The Regge trajectories are plotted in Fig. 6(b), showing the trajectories $n=5$ and $n=2$ that, respectively, pass near Re $L=1$ and 3 and, therefore are responsible for the shape resonance and the bound state of the negative Sm^- ion.

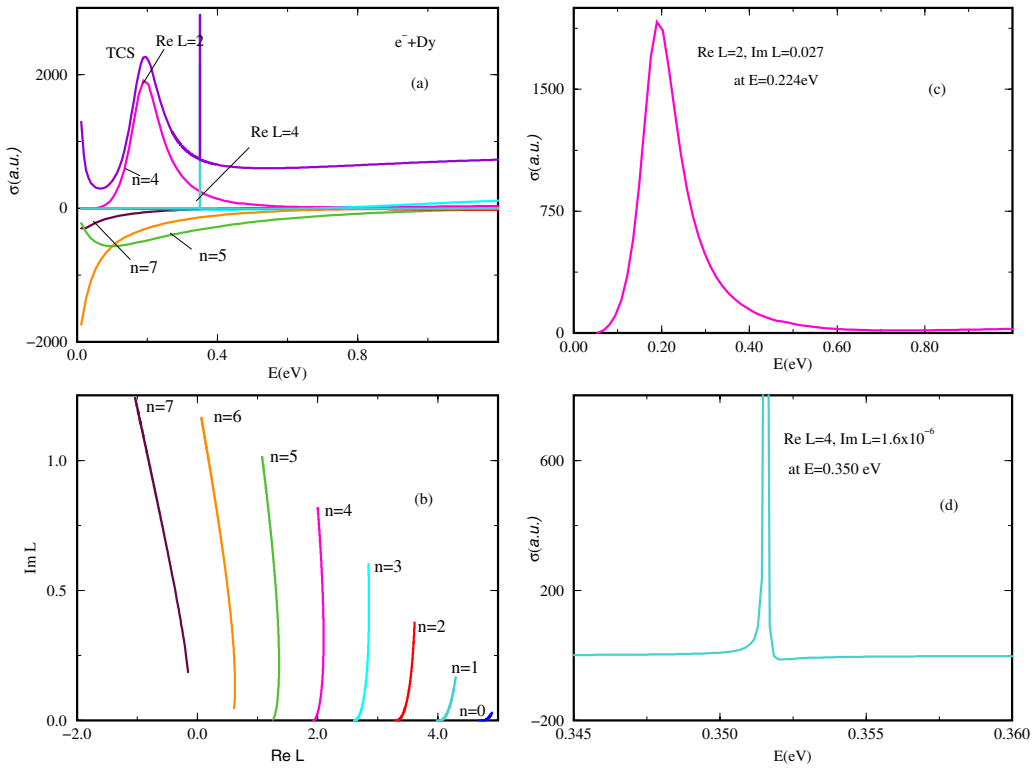

FIG. 10. (Color online) (a) The same as in Fig. 1(a) except that the results are for e^--Dy scattering versus E (eV); note the Wigner threshold behavior of the TCS, which is clearly determined by the $n=5$ Mulholland partial cross section and the RT minimum near threshold. (b) Regge trajectories, viz., Im $L(E)$ versus Re $L(E)$, for Dy^-, demonstrating the main Re $L(E)$ contributors to the TCS. (c) The same as in Fig. 1(b) except that the results are for e^--Dy scattering versus E (eV), corresponding to the Regge trajectory that passes near Re $L=2$ at $E=0.194$ eV, and hence responsible for the short-lived resonance with Im $L=0.027$ in the TCS at that energy. (d) The same as in Fig. 1(d) except that the results are for e^--Dy scattering versus E (eV), corresponding to the Regge trajectory that passes near Re $L=4$ at $E=0.3515$ eV, and hence responsible for the resonance with Im $L=1.6\times10^{-6}$ in the TCS at that energy. This is a long-lived resonance as seen by its large angular life $(\text{Im}\,L)^{-1}$.

G. Electron scattering from the Eu atom

The elastic scattering TCS and the Mulholland partial cross sections for the e^--Eu scattering are shown in Fig. 7(a) and they are similar to those for the e^--Sm scattering presented above. Figures 7(c) and 7(d) present, respectively, the expanded views of the shape resonance at 0.029 eV and the Mulholland contribution to the total cross section, in a.u., for the e^--Eu scattering versus E (eV), corresponding to the Regge trajectory that passes near Re $L=3$ [see Fig. 7(b)] at $E=0.116$ eV. Because of its small Im $L=7.6\times10^{-6}$ the resonance in Fig. 7(d) is identified with the EA of the Eu atom and the electron attachment corresponds to Re $L=3$. As seen from Table II, the available measurements [32,26] disagree between themselves, with the Davis and Thompson measurement being much higher, including that with the present value. However, the agreement between our EA and the most recently calculated value of 0.117 eV [78]. is indeed outstanding. In Fig. 7(b) is plotted Im L versus Re L, showing the main trajectories contributing to the resonances of Figs. 7(c) and 7(d).

H. Electron scattering from the Gd atom

Figure 8(a) presents the elastic scattering TCS and the Mulholland partial cross sections for the e^--Gd scattering; they clearly resemble those of Fig. 7. The expanded view of Fig. 8(c) shows the parameters of the shape resonance, viz., Re $L=1$, Im $L=0.030$, and $E=0.034$ eV. Figure 8(d) displays a closer look at the Mulholland contribution to the total cross section, in a.u., for the e^--Gd scattering versus E (eV), corresponding to the Regge trajectory ($n=1$) that passes near Re $L=3$ [see Fig. 8(b)] with Im $L=1.2\times10^{-5}$ at $E=0.137$ eV. The small value of Im L for this system leads us to identify this long-lived resonance with the EA of the Gd atom. There is only one measurement to compare our calculation with; however, it only determined the lower limit of the EA as >0.1 eV [26]. Figure 8(b) presents the Regge trajectories, again clearly demonstrating that the trajectories ($n=4$ and $n=1$) that, respectively, pass near Re $L=1$ and Re $L=3$ are the important ones.

Interestingly, the value of the b parameter for Gd is larger than the values of the other lanthanides, except for the La, Ce, and Pr atoms. Here we note the configuration of Gd, viz., $[\text{Xe}]\,4f^7 5d6s^2$. Therefore, the importance of the polarization interaction is critical and results in significant changes in the EA of Gd in comparison with that of Eu above (see also Table I for the values of b).

I. Electron scattering from the Tb atom

Figure 9(a) presents the near-threshold elastic scattering TCS and the Mulholland partial cross sections for the e^--Tb

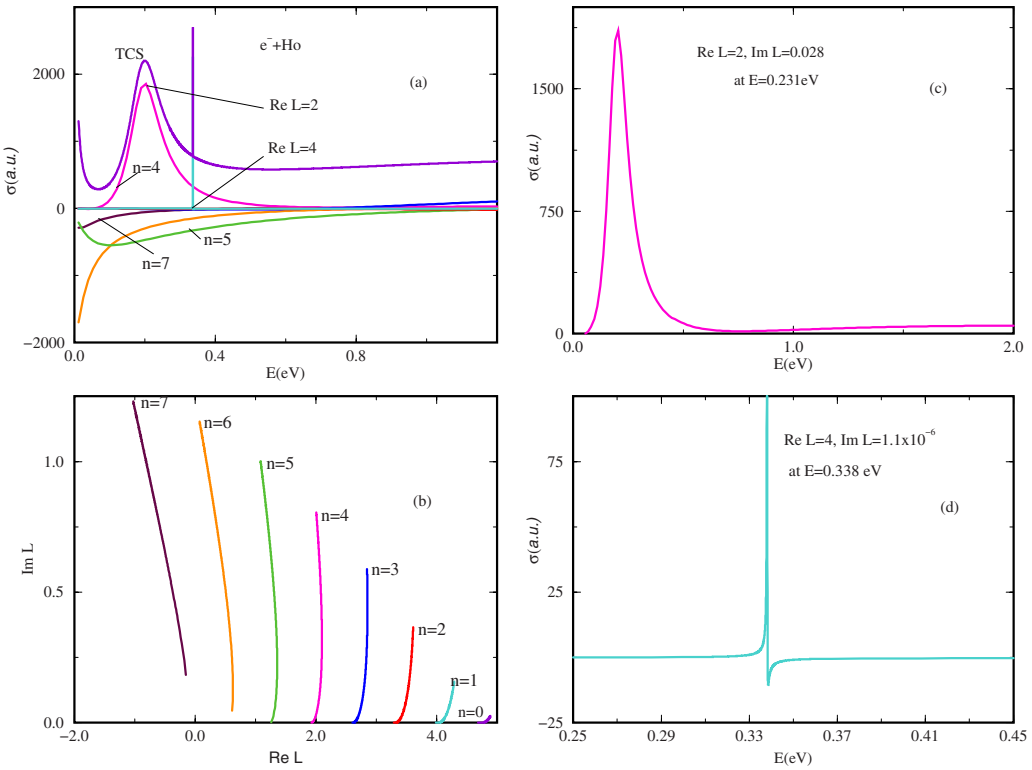

FIG. 11. (Color online) (a) The same as in Fig. 1(a) except that the results are for e^--Ho scattering versus E (eV). Note the Wigner threshold behavior of the TCS, which clearly is determined by the $n=5$ Mulholland partial cross section and the RT minimum near threshold. (b) Regge trajectories, viz., Im $L(E)$ versus Re $L(E)$, for Ho^-, demonstrating the main Re $L(E)$ contributors to the TCS. (c) The same as in Fig. 1(b) except that the results are for e^--Ho scattering versus E (eV), corresponding to the Regge trajectory that passes near Re $L=2$ at $E=0.231$ eV, and hence responsible for the short-lived resonance determined by Im $L=0.028$ in the TCS at that energy. (d) The same as in Fig. 1(d) except that the results are for e^--Ho scattering versus E (eV), corresponding to the Regge trajectory that passes near Re $L=4$ at $E=0.338$ eV, and hence responsible for the resonance determined by Im $L=1.1\times10^{-6}$ in the TCS at that energy. This is a long-lived resonance as seen by its large angular life $(\text{Im}\,L)^{-1}$.

scattering. We note that here the near-threshold resonance structure is pulled toward the higher E value in comparison with the case of the e^--Gd scattering, thereby revealing the RT minimum at about 0.068 eV and the Wigner threshold behavior, which corresponds to the $n=5$ Mulholland partial cross section. Here the nonzero RT minimum arises from the interference between the $n=4$ and $n=5$ Mulholland partial cross sections. The results in this case differ from those of Fig. 8(a) and closely resemble those of Fig. 1(a). Figure 9(c) exhibits the expanded view of the shape resonance whose parameters are Re $L=2$, Im $L=0.032$, and $E=0.231$ eV. Figure 9(d) displays the expanded view of the Mulholland contribution to the total cross section, in a.u., for the e^--Pm scattering versus E (eV), corresponding to the Regge trajectory that passes near Re $L=4$ [see Fig. 9(b)] with Im $L=5.0\times10^{-6}$ at $E=0.436$ eV. This dramatic resonance, characterized by the usual small value of Im L is identified with the EA of Tb.

We note that the atomic structure of Tb leads to electron attachment to a Re $L=4$ at a larger E value similar to the case of the e^--La scattering. Again here our EA value of 0.436 eV disagrees significantly with that measured by Davis and Thompson [28] whose value is >1.165 eV as well as with that of Ref. [26], which gives an EA >0.1 eV. The latest theoretical value [78]. is smaller than our value by a factor of approximately 5. Here it must be pointed out that Ref. [78]. assumed a p-electron attachment for all the lanthanides in calculating their BE's. In our calculation no such an assumption is made; the results simply come directly out of the Regge calculation. The Regge trajectories are presented in Fig. 9(b), with their usual interpretation; the shape resonance is determined by the $n=4$ trajectory while the $n=1$ trajectory defines the bound state of the Pm^- ion.

J. Electron scattering from the Dy atom

The near-threshold resonance structure in the cross sections, shown in Fig. 10(a), for the e^--Dy scattering resembles that of the e^--Tb scattering. The RT minimum is at about 0.068 eV, formed through the interference between the $n=4$ and $n=5$ Mulholland partial cross sections. The Wigner threshold behavior is determined by the $n=5$ Mulholland partial cross section. Figure 10(c) gives the close view of the shape resonance whose parameters are Re $L=2$, Im $L=0.027$, and $E=0.194$ eV. Figure 10(d) presents the expanded view of the Mulholland contribution to the total cross section, in a.u., for the e^--Dy scattering versus E (eV), corresponding to the Regge trajectory that passes near Re $L=4$ [see Fig. 10(b)] with Im $L=1.6\times10^{-6}$ at $E=0.3515$ eV. This resonance, characterized by a very small value of Im L compared to that of the shape resonance above, is identified with the EA of the Dy atom; the electron attachment in this case is

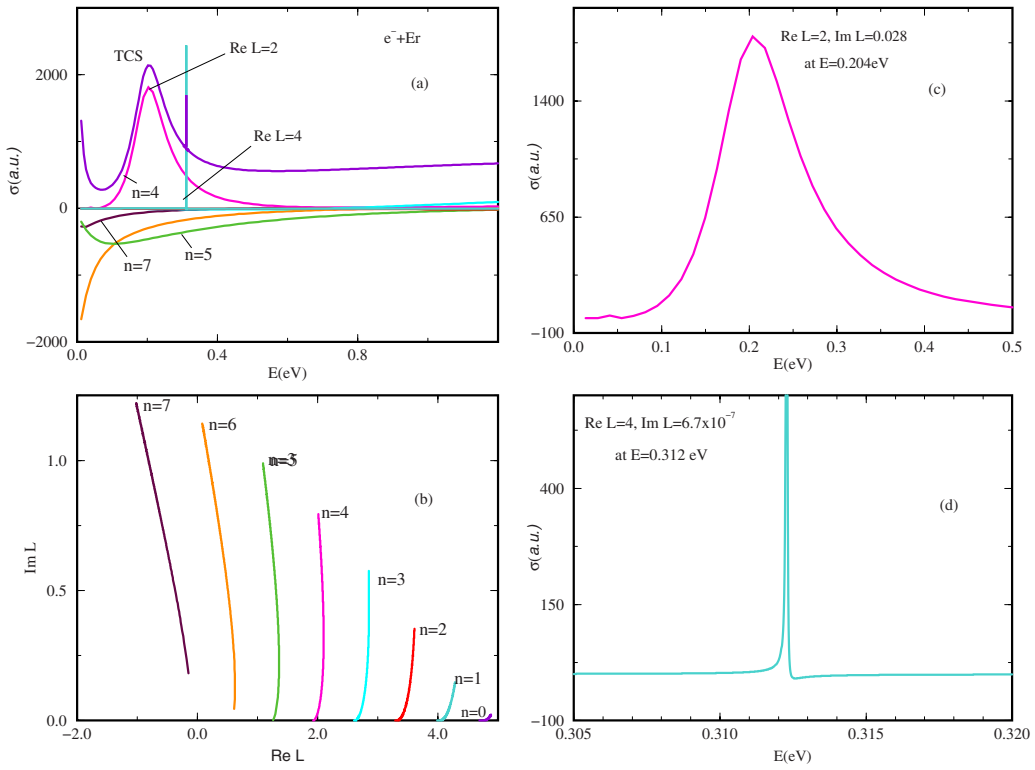

FIG. 12. (Color online) (a) The same as in Fig. 1(a) except that the results are for e^--Er scattering versus E (eV); note the Wigner threshold behavior of the TCS, which clearly is determined by the $n=5$ Mulholland partial cross section and the RT minimum near threshold. (b) Regge trajectories, viz., Im $L(E)$ versus Re $L(E)$, for Er^-, demonstrating the main Re $L(E)$ contributors to the TCS. (c) The same as in Fig. 1(b) except that the results are for e^--Er scattering versus E (eV), corresponding to the Regge trajectory that passes near Re $L=2$ at $E=0.204$ eV, and hence responsible for the short-lived resonance defined by Im $L=0.028$ in the TCS at that energy. (d) The same as in Fig. 1(d) except that the results are for e^--Er scattering versus E (eV), corresponding to the Regge trajectory that passes near Re $L=4$ at $E=0.312$ eV, and hence responsible for the resonance defined by Im $L=6.7\times1^{-7}$ in the TCS at that energy.

also to a Re $L=4$. The only available EA value for the Dy atom to compare with is 0.015(3) [24], which is several orders of magnitude smaller than our calculated value. In Fig. 10(b) is plotted the Regge trajectories for the e^--Dy scattering, demonstrating that indeed the trajectories passing near Re $L=2$ and Re $L=4$ are responsible for the resonances in the cross sections; these trajectories are, respectively, the $n=4$ and $n=1$.

K. Electron scattering from the Ho atom

For the e^--Ho scattering results [Fig. 11(a),] the near-threshold resonance structure resembles that of the e^--Dy scattering. The RT minimum is predicted to be at 0.070 eV, while the Wigner threshold behavior follows the $n=5$ Mulholland partial cross section. The RT minimum is generated through the interference between the $n=4$ and $n=5$ Mulholland partial cross sections, leading to a nonzero minimum. The parameters of the shape resonance, shown in the expanded Fig. 11(c) are calculated to be Re $L=2$, Im $L=0.028$, and $E=0.231$ eV. These can be contrasted with those of Fig. 11(d), viz., Re $L=4$, Im $L=1.1\times10^{-6}$, and $E=0.338$ eV. Note that for this resonance Im L is also several orders of magnitude smaller than the Im L value for the shape resonance. This resonance is identified with the EA of the Ho atom and the electron attachment is to Re $L=4$. Clearly, it is only through the close scrutiny of Im L that the shape resonance and the bound state of the negative ion can be differentiated unambiguously, particularly that their energies are close together. The only available experimental estimate to compare with gives the value of EA <0.005 eV [24]. There are no other theoretical calculations available for this atom; this further manifests the difficulties of calculating reliable EA values for the lanthanides. Figure 11(b) displays the Regge trajectories demonstrating that the Re $L=2$ and Re $L=4$ are responsible for the resonances in the cross sections; they are generated by the $n=4$ and $n=1$ trajectories, respectively.

L. Electron scattering from the Er atom

The near-threshold resonance structure in the total cross section for the e^--Er scattering is shown in Fig. 12(a) and resembles those for the e^--Ho and e^--Dy scattering. The Wigner threshold behavior is determined by the $n=5$ Mulholland partial cross section, while the RT minimum appears at $E=0.075$ eV, due to the interference between the $n=4$ and $n=5$ Mulholland partial cross sections. The expanded view of the shape resonance is shown in Fig. 12(c) and its parameters are Re $L=2$, Im $L=0.028$, and $E=0.204$ eV. Figure 12(d) displays the long-lived resonance as distinguished from the shape resonance by its very small Im $L=6.7$

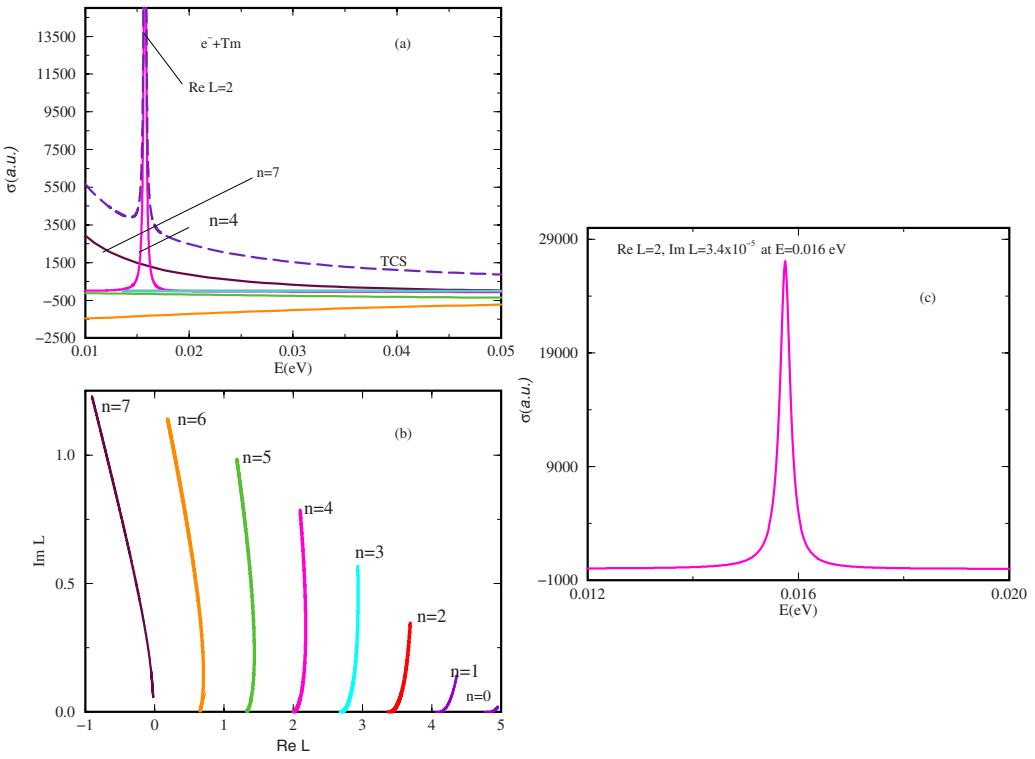

FIG. 13. (Color online) (a) The same as in Fig. 1(a) except that the results are for e^--Tm scattering versus E (eV); the RT minimum and the Wigner threshold behavior of the TCS are clearly visible, with the latter being determined by the $n=7$ Mulholland partial cross section. (b) Regge trajectories, viz., Im $L(E)$ versus Re $L(E)$, for Tm^-, demonstrating the main Re $L(E)$ contributors to the TCS. (c) The same as in Fig. 1(d) except that the results are for e^--Tm scattering versus E (eV), corresponding to the Regge trajectory that passes near Re $L=2$ at $E=0.016$ eV, and hence responsible for the resonance with Im $L=3.4\times10^{-5}$ in the TCS at that energy. This long-lived resonance is seen from its large angular life $(\text{Im}\, L)^{-1}$.

$\times 10^{-7}$ and is identified with the EA of the Er atom with the value of 0.312 eV and Re $L=4$. The Mulholland contribution to the total cross section, in a.u., for the e^--Er scattering versus E (eV), corresponds to the Regge trajectory that passes near Re $L=4$ [see Fig. 12(b)]. The electron attachment in this case is to a Re $L=4$. The only available experimental estimate to compare with gives the value of EA <0.005 eV [24]. The Regge trajectories for the e^--Er scattering are plotted in Fig. 12(b) demonstrating that indeed Re $L=2$ and Re $L=4$ are responsible for the resonances in the TCS and the Mulholland partial cross sections.

M. Electron scattering from the Tm atom

For the e^--Tm scattering the near-threshold resonance structure in the total cross section, shown in Fig. 13(a), is significantly different from those of parts (a) in Figs. 1–12. Clearly the Wigner threshold behavior corresponds to the $n=7$ Mulholland partial cross section, while the RT minimum is at about 0.014 eV and is determined by the interference between the $n=4$ and $n=7$ Mulholland partial cross sections. Contrary to the case of the e^--Er scattering, for example, shown in Fig. 12(a), the very close to threshold resonance in e^--Tm scattering is determined by the parameters Re $L=2$, Im $L=3.4\times10^{-5}$, and $E=0.016$ eV [see expanded view in Fig. 13(c)]. The Mulholland contribution to the TCS, in a.u., for the e^--Tm scattering versus E (eV), corresponds to the Regge trajectory that passes near Re $L=2$ [see Fig. 13(c)]. This resonance, characterized by a very small value of Im L is identified with the EA of the Tm atom. In the e^--Tm scattering the positions of the long-lived resonance and the shape resonance have switched around their positions in comparison to those of Figs. 1–12.

Note that here we do not show the shape resonance because its position is at a value of E greater than the 1 eV of interest in this paper and its Im L is orders of magnitude greater than that for the resonance corresponding to the EA in Fig. 13(c). This EA value for the Tm atom represents the lowest among the lanthanides and should be compared with the measured values of 1.029(22) eV by Davis and Thompson [28] and of 0.032(7) eV [24] and the theoretical values of 0.02–0.136 eV [39]. We note that the EA values of Refs. [39,24] are about a factor of 2 larger than our value while the Davis and Thompson [28] value is about two orders of magnitude larger than our EA and of the rest. In this case the Regge trajectories, shown in Fig. 13(b), simply demonstrate the contribution from the $n=3$ trajectory with Re $L=2$ to the resonance, corresponding to the EA of the Tm atom.

N. Electron scattering from the Yb atom

The near-threshold resonance structure in the e^--Yb scattering TCS and the Mulholland partial cross sections presented in Fig. 14(a) is also characterized by a Wigner threshold behavior determined by the $n=6$ Mulholland partial cross section, followed by a RT minimum in the TCS at about

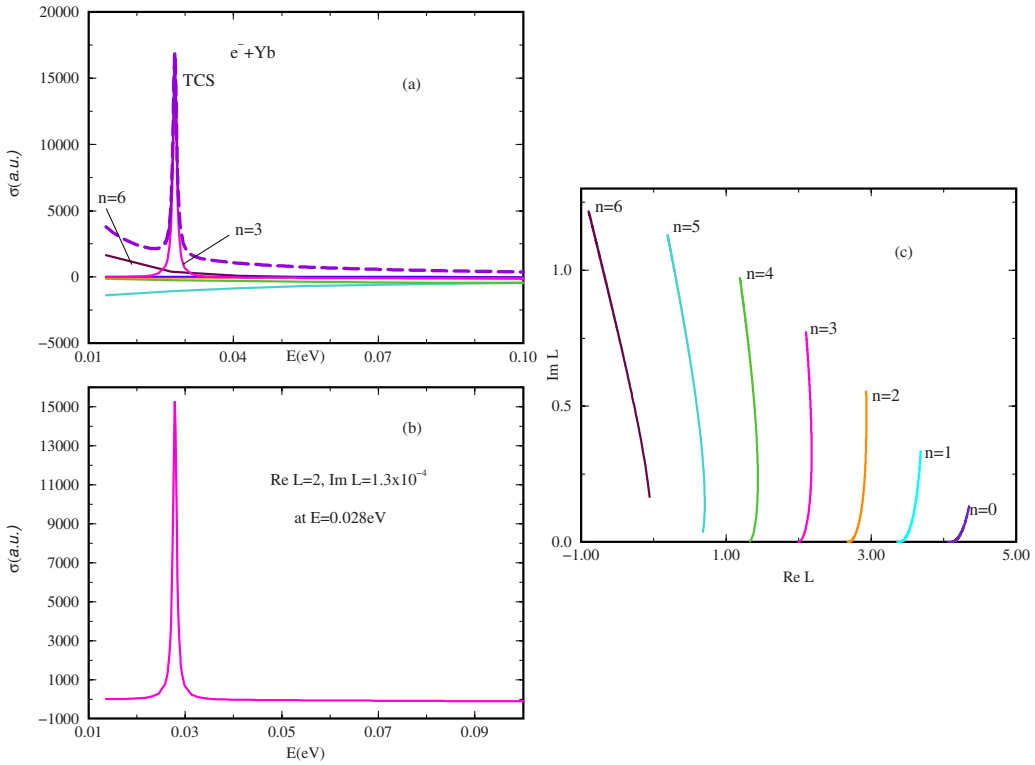

FIG. 14. (Color online) (a). The same as in Fig. 1(a) except that the results are for e^--Yb scattering versus E (eV). Note the Wigner threshold behavior of the TCS, which clearly is determined by the $n=6$ Mulholland partial cross section and the RT minimum near threshold. (b) The same as in Fig. 1(d) except that the results are for e^--Yb scattering versus E (eV), corresponding to the Regge trajectory that passes near $\mathrm{Re}\,L=2$ at $E=0.028$ eV, and hence responsible for the resonance ($\mathrm{Im}\,L=1.3\times10^{-4}$) in the TCS at that energy. This is a long-lived resonance as seen by its large angular life $(\mathrm{Im}\,L)^{-1}$. (c) Regge trajectories, viz., $\mathrm{Im}\,L(E)$ versus $\mathrm{Re}\,L(E)$, for Yb^-, demonstrating the main $\mathrm{Re}\,L(E)$ contributors to the TCS.

0.0236 eV and greatly resembles that of the e^--Tm scattering displayed in Fig. 13(a). The RT minimum is generated through the interference between the $n=3$ and $n=6$ Mulholland partial cross sections, resulting in its nonzero value. We note that this value differs from the true RT minimum, defined by where the $n=6$ Mulholland partial cross section crosses the real axis. Figure 14(b) shows an expanded view of the resonance whose parameters are $\mathrm{Re}\,L=2$, $\mathrm{Im}\,L=1.3\times10^{-4}$, and $E=0.028$ eV, demonstrating the Mulholland contribution to the TCS, in a.u., in the e^--Yb scattering versus E (eV); the Regge trajectory that passes near $\mathrm{Re}\,L=2$ [see Fig. 14(c)], is thus responsible for this resonance. Because of its small value of $\mathrm{Im}\,L$ we identify this resonance with the EA of the Yb atom. This value, much smaller than that of the shape resonance, not displayed because it is at an energy value greater than 1 eV, should be compared with those in Table II. Those values vary from the near zero EA value of less than 3 meV [52] to a high value of 0.0985 eV [42]. The large spread in the tabulated EA values calls for further careful experimental and theoretical investigations as was done for the Ca^- negative ion.

Kelemen *et al.* [79] calculated the elastic scattering cross sections of electrons by Ca, Sr, Ba, and Yb atoms in the electron impact energy range 0–200 eV. They used the EA value of 0.054 ± 0.027 eV for the Yb atom from Ref. [41] and found a RT minimum in the elastic cross section of 0.012 eV, arising from the s-wave partial cross section. This value can be compared with that obtained here of 0.0236 eV, which is a factor of about 2 larger. We note, however, that Kelemen *et al.* began their calculations at 0.1 eV and found that the s-, p- and d-partial cross sections are the main contributors to the integral elastic cross section in the energy range between zero and about 1.2 eV, with the d-partial cross section dominating the elastic cross section around the maximum at about 1.2 eV. In contrast, here we found a $\mathrm{Re}\,L=3$ shape resonance at about 1.60 eV, with $\mathrm{Im}\,L=0.13$ (result not shown for the same reason as above).

O. Electron scattering from the Lu atom

The electronic structure of Lu is $[\mathrm{Xe}]4f^{14}5d6s^2$ and resembles that for the La atom, except that the latter has no $4f$ subshell in its structure. However, its near-threshold elastic TCS resembles that for the e^--Yb scattering, thus demonstrating the importance of the $4f$ subshell in the scattering process. The TCS and the Mulholland partial cross sections for the e^--Lu scattering are presented in Fig. 1 of Ref. [66] and discussed there; they will not be reproduced here. Just as in Fig. 14(a) above the total cross section is characterized by a Wigner threshold behavior determined by the $n=6$ Mulholland partial cross section, followed by a RT minimum at about 0.025 eV. The RT minimum results from the interference between the $n=3$ and $n=6$ Mulholland partial cross sections. As in the case of the e^--Yb scattering, this minimum differs from the true RT minimum, defined by the value of E where the $n=6$ Mulholland partial cross section crosses

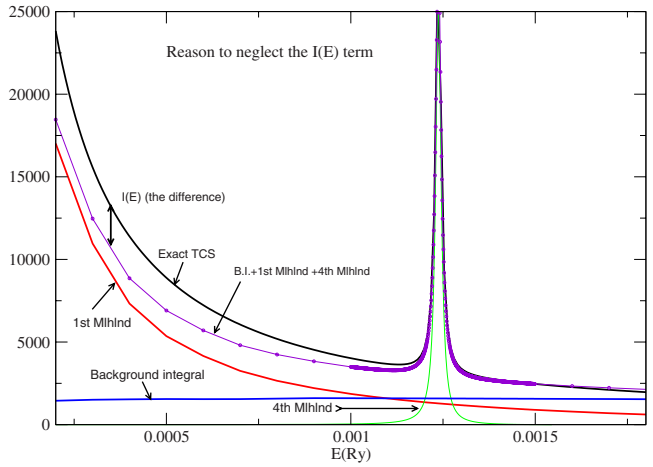

FIG. 15. (Color online) Total cross section (labeled TCS) and the various contributions to it stemming from the discrete sum in the Mulholland formula for e^--Hf scattering demonstrating the unimportance of the $I(E)$ term in Eq. (1).

the real axis. The resonance corresponding to the attachment of a Re $L=2$ electron at $E=0.029$ eV defines the bound state of the Lu^- negative ion formed during the collision. The angular life of this resonance is proportional to Im $L=1.4\times10^{-4}$, indicating the existence of a stable bound state of the Lu^- ion. The parameters of the resonance are close to those of the e^--Yb scattering, including the EA. Our EA value of Lu differs significantly from that of Davis and Thompson [29] and from the existing theoretical values [43,45]. The AMS measurement [26] only provided the lower limit of the EA of Lu. The shape resonance in the e^--Lu scattering is at a higher value of the impact energy of interest in this paper.

P. Justification of the neglect of the $I(E)$ term in the Mulholland formula: Example from e^--Hf scattering

In this section we justify the neglect of the $I(E)$ term in the Mulholland formula, Eq. (1), using the e^--Hf scattering as an example [66]. The different curves in Fig. 15 represent the total cross section (labeled TCS) and the various contributions to the TCS stemming from the discrete sum in the Mulholland formula. This sum is over poles of the S matrix in the complex angular momentum plane. In a sense, this sum can be thought of as the equivalent of the various partial waves in the traditional partial wave expansion over integer angular momentum l, albeit a sum with considerably fewer members than the latter. We can therefore refer to the various contributions as Mulholland partial cross sections to differentiate them from the standard definition of partial cross sections referred to in the published literature.

The first (integral) term is the smooth impact parameter-type contribution to the total cross section (background term). It represents the difference between the TCS and the sum over all the Mulholland partial contributions [since $I(E)$ is neglected here]. This explains why graphically, the TCS curve is "translated" vertically upward. We also see from the figure that the $I(E)$ term does not affect the position of the RT minimum. In the figure, B.I. stands for background integral and Mlhlnd stands for Mulholland.

IV. SUMMARY AND CONCLUSIONS

In this paper we have employed the recently developed Regge-pole methodology [56], wherein is embedded the vital electron correlation effects, together with a Thomas-Fermi-type potential that incorporates the crucial polarization interaction, to explore low energy ($E\leqslant1$ eV) electron elastic scattering from the lanthanides, La through Lu. The Mulholland partial cross sections and the TCS's for electron elastic scattering have been calculated. Dramatically sharp resonances have been found to characterize the near-threshold electron elastic scattering from these atoms, whose energy positions have been identified with the EA's of these atoms through the careful scrutiny of the imaginary part of the complex angular momentum L. For shape resonances Im L is roughly of the order of 10^{-2}, while Im L for the BE's is several orders of magnitude smaller than the corresponding value for the shape resonances. This enables the unambiguous identification of the BE's from the resonance structures in the TCS's. Shape resonances, Ramsauer-Townsend minima, and the Wigner threshold behavior have been determined as well.

We have compared our calculated EA's with various experimental and theoretical values where these are available. However, very low-energy electron scattering data for many of the lanthanides are unavailable and most of the cross sections presented here are generally the first ever, including the corresponding EA values. Many of the available experimental and theoretical EA's vary significantly from one another (see, for example, the EA's of Ce and Yb in Table II). We also note from the same table that the EA values of Davis and Thompson tend to be larger by comparison than the rest of the data. Additionally, most of the experimental data in the table give mainly lower and upper limits to the EA values. We would like to see more definitive EA values for many of the experimental EA's. Admittedly, the experiments are very difficult to perform and many previous theoretical calculations are riddled with uncertainties because of the complex and subtle interactions among the very many diverse electron configurations involved.

After we completed this investigation, the paper [78] appeared. The authors calculated only the BE's of many of the lanthanide anions using the MCDF-RCI method, assuming a $6p$ electron attachment for all the anions; there were no cross sections calculated by these authors. Our method is completely different from that of O'Malley and Beck [78] and does not assume any specific orbital attachment for the extra electron; the value of the resonant Re L comes directly from the calculation and the EA's are extracted from the resonances in the cross sections rather than from structure calculations. Where the shape resonances precede the stable bound states of the negative ions in the TCS's the agreement between the EA's of O'Malley and Beck [78] and ours varies from good to outstanding. However, in cases where the RT minima and the shape resonances come before the bound ionic state, the O'Malley and Beck BE's are lower than ours by factors varying from about 5 to 8. We believe that the source of this significant discrepancy originates from the assumed $6p$ electron attachment for all the lanthanide atoms by O'Malley and Beck [78]. Interestingly, there is reasonable

agreement between the O'Malley and Beck [78] and our BE for the Tm^- ion, including that it forms a tenuously bound state.

We conclude by quoting Geltman, "Resonance is given many meanings in the literature, leading to much confusion" [80]. Here we have employed the rigorous definition of resonances as singularities of the S matrix to extract unambiguous BE's through close scrutiny of the Im L, even to distinguish between shape resonances and BE's. We believe that our results are reliable as evidenced by the agreements between our calculated values of the EA's of the La, Ce, Nd, Eu, and Tm atoms when compared with the latest measured [27,53] and calculated [36,55,78] data.

ACKNOWLEDGMENTS

This work was supported by U.S. DOE, Division of Chemical Sciences, Office of Basic Energy Sciences, Office of Energy Research, and the CAU CFNM funded by NSF-CREST Program. D.S. is supported through an EPSRC (UK) grant. We thank Dr. S. T. Manson and Dr. N. Deb for valuable discussions. The computing facilities at the Queen's University of Belfast are greatly appreciated.

[1] C. F. Fischer, J. B. Lagowski, and S. H. Vosko, Phys. Rev. Lett. **59**, 2263 (1987).
[2] D. J. Pegg, J. S. Thompson, R. N. Compton, and G. D. Alton, Phys. Rev. Lett. **59**, 2267 (1987).
[3] K. W. McLaughlin and D. W. Duquette, Phys. Rev. Lett. **72**, 1176 (1994).
[4] V. V. Petrunin, H. H. Andersen, P. Balling, and T. Andersen, Phys. Rev. Lett. **76**, 744 (1996).
[5] D. R. Bates, Adv. At., Mol., Opt. Phys. **27**, 1 (1991); C. Blondel, Phys. Scr., T **58**, 31 (1995).
[6] T. Andersen, Phys. Rep. **394**, 157 (2004).
[7] D. J. Pegg, Rep. Prog. Phys. **67**, 857 (2004).
[8] S. T. Buckman and C. W. Clark, Rev. Mod. Phys. **66**, 539 (1994).
[9] H. Hotop, M.-W. Ruf, and I. I. Fabrikant, Phys. Scr., T **110**, 22 (2004).
[10] S. Zivanov, B. C. Ibanescu, M. Paech, M. Poffet, P. Baettig, A.-C. Sergenton, S. Grimme, and M. Allan, J. Phys. B **40**, 101 (2007).
[11] R. V. Krems, A. Dalgarno, N. Balakrishnan, and G. C. Groenenboom, Phys. Rev. A **67**, 060703(R) (2003).
[12] A. J. Kerman, J. M. Sage, S. Sainis, T. Bergeman, and D. DeMille, Phys. Rev. Lett. **92**, 033004 (2004).
[13] S. Aubin, S. Myrskog, M. H. T. Extavour, L. J. LeBlanc, D. McKay, A. Stummer, and J. H. Thywissen, Nat. Phys. **2**, 384 (2006).
[14] E. P. Wigner, Phys. Rev. **73**, 1002 (1948).
[15] T. Andersen, H. K. Haugen, and H. Hotop, J. Phys. Chem. Ref. Data **28**, 1511 (1999).
[16] M. Reicherts, T. Roth, A. Gopalan, M.-W. Ruf, H. Hotop, C. Desfrancois, and I. I. Fabrikant, Europhys. Lett. **40**, 129 (1997).
[17] I. I. Fabrikant and V. S. Lebedev, J. Phys. B **33**, 1521 (2000); I. I. Fabrikant, *ibid.* **31**, 2921 (1998).
[18] S. Danzenbächer, Y. Kucherenko, C. Laubschat, D. V. Vyalikh, Z. Hossain, C. Geibel, X. J. Zhou, W. L. Yang, N. Mannella, Z. Hussain, Z. X. Shen, and S. L. Molodtsov, Phys. Rev. Lett. **96**, 106402 (2006).
[19] O. Eriksson, M. Cahay, and J. M. Wills, Phys. Rev. B **65**, 033304 (2001).
[20] A. Nie, J. Wu, C. Zhou, S. Yao, C. Luo, R. C. Forrey, and H. Cheng, Int. J. Quantum Chem. **107**, 219 (2006).
[21] V. T. Davis, J. S. Thompson, and A. Covington, Nucl. Instrum. Methods Phys. Res. B **241**, 118 (2005).
[22] M. A. Garwan, A. E. Litherland, M. J. Nadeau, and X. L. Zhao, Nucl. Instrum. Methods Phys. Res. B **79**, 631 (1993).
[23] D. Berkovits, E. Boaretto, O. Heber, G. Hollos, G. Korschinek, W. Kutschera, and M. Paul, Nucl. Instrum. Methods Phys. Res. B **92**, 254 (1994).
[24] M. J. Nadeau, A. E. Litherland, M. A. Garwan, and X. L. Zhao, Nucl. Instrum. Methods Phys. Res. B **92**, 265 (1994).
[25] D. Berkovits, S. Ghelberg, O. Heber, and M. Paul, Nucl. Instrum. Methods Phys. Res. B **123**, 515 (1997).
[26] M. J. Nadeau, M. A. Garwan, X. L. Zhao, and A. E. Litherland, Nucl. Instrum. Methods Phys. Res. B **123**, 521 (1997).
[27] A. M. Covington, D. Calabrese, J. S. Thompson, and T. J. Kvale, J. Phys. B **31**, L855 (1998).
[28] V. T. Davis and J. S. Thompson, Phys. Rev. A **65**, 010501(R) (2001).
[29] V. T. Davis and J. S. Thompson, J. Phys. B **34**, L433 (2001).
[30] V. T. Davis and J. S. Thompson, Phys. Rev. Lett. **88**, 073003 (2002).
[31] V. T. Davis and J. S. Thompson, J. Phys. B **35**, L11 (2002).
[32] V. T. Davis and J. S. Thompson, J. Phys. B **37**, 1961 (2004).
[33] S. M. O'Malley and D. R. Beck, J. Phys. B **38**, 2645 (2005).
[34] S. M. O'Malley and D. R. Beck, Phys. Rev. A **60**, 2558 (1999).
[35] X. Cao and M. Dolg, Phys. Rev. A **69**, 042508 (2004).
[36] S. M. O'Malley and D. R. Beck, Phys. Rev. A **74**, 042509 (2006).
[37] S. M. O'Malley and D. R. Beck, Phys. Rev. A **61**, 034501 (2000).
[38] K. Dinov and D. R. Beck, Phys. Rev. A **51**, 1680 (1995).
[39] J. A. Chevary and S. H. Vosko, J. Phys. B **27**, 657 (1994).
[40] S. M. O'Malley and D. R. Beck, Phys. Rev. A **70**, 022502 (2004).
[41] S. H. Vosko, J. A. Chevary, and I. L. Mayer, J. Phys. B **24**, L225 (1991).
[42] A. A. Gribakina, G. F. Gribakin, and V. K. Ivanov, Phys. Lett. A **168**, 280 (1992).
[43] E. Eliav, U. Kaldor, and Y. Ishikawa, Phys. Rev. A **52**, 291 (1995).
[44] E. N. Avgoustoglou and D. R. Beck, Phys. Rev. A **57**, 4286 (1998).
[45] S. H. Bosko and J. A. Chevary, J. Phys. B **26**, 873 (1993).
[46] S. H. Vosko, J. B. Lagowski, I. L. Mayer, and J. A. Chevary,

Phys. Rev. A **43**, 6389 (1991).
[47] V. A. Dzuba and G. F. Gribakin, Phys. Rev. A **49**, 2483 (1994).
[48] V. A. Dzuba and G. F. Gribakin, Phys. Rev. A **55**, 2443 (1997).
[49] V. A. Dzuba and G. F. Gribakin, J. Phys. B **31**, L483 (1998).
[50] E. N. Avgoustoglou and D. R. Beck, Phys. Rev. A **55**, 4143 (1997).
[51] K. D. Dinov, D. R. Beck, and D. Datta, Phys. Rev. A **50**, 1144 (1994).
[52] H. H. Andersen, T. Andersen, and U. V. Pedersen, J. Phys. B **31**, 2239 (1998).
[53] C. W. Walter, N. D. Gibson, C. M. Janczak, K. A. Starr, A. P. Snedden, R. L. Field III, and P. Andersson, Phys. Rev. A **76**, 052702 (2007).
[54] Z. Felfli, A. Z. Msezane, and D. Sokolovski, J. Phys. B **41**, 041001 (2008).
[55] S. M. O'Malley and D. R. Beck, Phys. Rev. A **77**, 012505 (2008).
[56] D. Sokolovski, Z. Felfli, S. Y. Ovchinnikov, J. H. Macek, and A. Z. Msezane, Phys. Rev. A **76**, 012705 (2007).
[57] S. C. Frautschi, *Regge Poles and S-matrix Theory* (W. A. Benjamin, New York, 1963).
[58] V. de Alfaro and T. Regge, *Potential Scattering* (North-Holland, Amsterdam, 1965).
[59] J. H. Macek, P. S. Krstic', and S. Yu. Ovchinnikov, Phys. Rev. Lett. **93**, 183203 (2004).
[60] Z. Felfli, A. Z. Msezane, and D. Sokolovski, J. Phys. B **39**, L353 (2006).
[61] A. Z. Msezane, Z. Felfli, and D. Sokolovski, Chem. Phys. Lett. **456**, 96 (2008).
[62] A. Z. Msezane, Z. Felfli, and D. Sokolovski, J. Phys. Chem. A **112**, 1999 (2008).
[63] A. Z. Msezane, Z. Felfli, and D. Sokolovski, J. Phys. B **41**, 105201 (2008).
[64] D. Sokolovski, K. Sen, V. Aquilanti, S. Cavalli, and D. De Fazio, J. Chem. Phys. **126**, 084305 (2007).
[65] D. Sokolovski, A. Z. Msezane, Z. Felfli, S. Yu. Ovchinnikov, and J. H. Macek, Nucl. Instrum. Methods Phys. Res. B **261**, 133 (2007).
[66] Z. Felfli, A. Z. Msezane, and D. Sokolovski, Phys. Rev. A **78**, 030703(R) (2008).
[67] V. I. Lengyel, V. T. Navrotsky, and E. P. Sabad, *Resonance Phenomena in Electron-Atom Collisions* (Springer-Verlag, Berlin, 1992), Chap. 7.
[68] M. H. F. Bettega, C. Winstead, and V. McKoy, Phys. Rev. A **74**, 022711 (2006).
[69] V. V. Petrunin, J. D. Voldstad, P. Balling, P. Kristensen, T. Andersen, and H. K. Haugen, Phys. Rev. Lett. **75**, 1911 (1995).
[70] J. Wu and J. Yuan, J. Phys. B **39**, 2493 (2006).
[71] H. W. van der Hart, C. Laughlin, and J. E. Hansen, Phys. Rev. Lett. **71**, 1506 (1993).
[72] V. V. Petrunin, H. H. Andersen, P. Balling, and T. Andersen, Phys. Rev. Lett. **76**, 744 (1996).
[73] H. P. Mulholland, Proc. Cambridge Philos. Soc. **24**, 280 (1928).
[74] L. H. Thomas, Proc. Cambridge Philos. Soc. **23**, 542 (1927); E. Fermi, Z. Phys. A: Hadrons Nucl. **48**, 73 (1928).
[75] S. Belov, N. B. Avdonina, Z. Felfli, M. Marletta, A. Z. Msezane, and S. N. Naboko, J. Phys. A **37**, 6943 (2004).
[76] J. N. L. Connor, J. Chem. Soc., Faraday Trans. **86**, 1627 (1990).
[77] P. G. Burke and C. Tate, Comput. Phys. Commun. **1**, 97 (1969).
[78] S. M. O'Malley and D. R. Beck, Phys. Rev. A **78**, 012510 (2008).
[79] V. I. Kelemen, E. Yu Remeta, and E. P. Sabad, J. Phys. B **28**, 1527 (1995).
[80] S. Geltman, *Topics in Atomic Collision Theory* (Krieger Publishing Company, Malabar, Florida, 1997).